





1 Deliverable administrative information

Deliverable number	5.2
Deliverable title	System model
Dissemination level	Public
Submission deadline	31/03/2025
Version number	2
Authors	PART (A) RISE (Sweden): Danilo Obradović, Mattias Persson, Mahantha Ampavatina Kambagiri, Erik Alvarez, Elnaz Abdollahi; PART (B) CERTH (Greece): Chairopoulos Nikolaos Charalampos, Giourka Paraskevi, Nikolopoulos Nikolaos, Petridis Stefanos, Rotas Renos, Valiakos Apostolos, Zornatzis Ioannis Athanasios, Salanova Grau Josep Maria, Athanasios Tolikas, Tamvakos Athanasios, Touliou Katerina, Grigoropoulos Konstantinos, Gkaidatzis Paschalis, Bintoudi Angelina, Ioannidis Dimosthenis.
Internal reviewers	First round, Part A: RISE (Sweden), CERTH (Greece), DBH (Hungary), and EMOBILITY SOLUTIONS (Hungary) Second round, with Part B: Within WP5.2
Document approval	Shreesha Vaidhya, RUPPRECHT CONSULT - Forschung & Beratung GmbH (Germany), Baerte de Brey, ElaadNL (Netherlands)

1.1 Legal Disclaimer

SCALE is funded by the European Union's Horizon Europe Research and Innovation programme under Grant Agreement No 101056874. The views represented in this document only reflect the views of the authors and not the views of the European Commission. The dissemination of this document reflects only the author's view and the European Commission is not responsible for any use that may be made of the information it contains.



2 Project Executive Summary

SCALE (Smart Charging Alignment for Europe) is a three-year Horizon Europe project that aims at preparing EU cities for mass deployment of electric vehicles and the accompanying smart charging infrastructure.

3 SCALE partners

List of participating cities:

- Oslo (NO)
- Rotterdam & Utrecht (NL)
- Eindhoven (NL)
- Toulouse (FR)
- Greater Munich Area (GER)
- Budapest & Debrecen (HU)
- Gothenburg (SE)

List of partners:

- (Coordinator) STICHTING ELAAD NL
- POLIS PROMOTION OF OPERATIONAL LINKS WITH INTEGRATED SERVICES, ASSOCIATION INTERNATIONALE POLIS BE
- GoodMoovs NL
- Rupprecht Consult Forschung & Beratung GmbH RC DE
- Trialog FR
- WE DRIVE SOLAR NL BV NL
- UNIVERSITEIT UTRECHT NL
- LEW Verteilnetz GmbH DE
- BAYERN INNOVATIV BAYERISCHE GESELLSCHAFT FUR INNOVATION UND WISSENSTRANSFER MBH DE
- ABB BV NL
- Enervalis BE
- GEMEENTE UTRECHT NL
- Equigy B.V. NL
- SONO MOTORS GMBH DE
- Meshcrafts As (Current) NO
- RISE Research Institutes of Sweden AB SE
- ETHNIKO KENTRO EREVNAS KAI TECHNOLOGIKIS ANAPTYXIS (CERTH) GR
- FIER Automotive FIER NL
- Emobility Solutions Kft. HU



- Serviced Office Belbuda Kft HU
- Enedis FR
- L'ASSOCIATION EUROPEENNE DE LA MOBILITE ELECTRIQUE (AVERE) BE
- Norsk elbilforening NO
- VDL ENABLING TRANSPORT SOLUTIONS BV NL
- Urban Electric Mobility Initiative UEMI DE
- Renault FR
- Chalmers University SE
- Polestar SE
- Hyundai NL NL

Social Links:



twitter.com/scaleproject_



www.linkedin.com/company/ scale-project-smart-charging-alignment-for-europe



www.youtube.com/channel/UC1HVFu5uJPCNSV96b3I_rcg

For further information please visit WWW.SCALE-HORIZON.EU



4 Deliverable executive summary

4.1 Key words

Electric Vehicles, Power system stability, V2G

4.2 Summary

WP5.2 focuses on analyzing some important aspects of the impact and opportunities of EV mass deployment in a power system grid. The analysis in PART A is divided into two key areas: local distribution grid voltage stability and Nordic power system frequency stability. In the local grid analysis, two real distribution networks were modeled using actual grid topologies, cable data, and smart meter information. The study examined the effects of smart charging strategies, comparing unidirectional (V1G) and bidirectional (V2G) charging. Using a cost-optimization algorithm, it assessed how different tariff structures influence charging behaviors and their impact on system loading and voltage stability in residential areas. At the Nordic power system level, the project evaluated frequency stability and the role of V2G in providing frequency control services. It analyzed frequency dynamics, identified key risks to stability, and simulated the potential impact of large-scale V2G frequency control. Additionally, the study investigated the effect of EV frequency control delays on system frequency and small-signal stability. By modeling dynamic responses to major disturbances, the project provides critical insights into the technical requirements needed for integrating EVs into frequency regulation services.

PART B focuses on the application of the Energy Planning Tool, developed and reported by CERTH as part of SCALE T2.6, in the pilot city of Gothenburg. The tool follows a three-step methodology: i) a transport model to extract mobility patterns of EV users, ii) an optimisation algorithm to identify optimal locations for V2G charger installation with the minimum possible grid congestion, and iii) a continuous-time system model evaluating interactions among the components of the proposed topology – namely, the EV battery, the V2G charger, and the local distribution grid (DN). To adjust to the specific requirements of T5.2 – mass adoption of V2G – nine different scenarios of possible EV user charging patterns were defined to reflect edge cases of the proposed methodology and assess various charging strategies. Moreover, a medium-voltage (MV) DN was selected to stress-test the scalability of the tool. Results confirm that the methodology can be extended to varying mobility conditions, supporting both the identification of the optimal charger locations and the dynamic operation of all interacting components within the system model.



It is astonishing to see that the distribution of EVs in the power system, together with their smart V2G strategies, can be quite supportive of grid operation in the sense of voltage and frequency stability aspects. The work results in WP5.2 show that for such a positive outcome, thorough analyses should be done in adequate power system models through carefully chosen test cases. The essential ingredient to valuable outcomes relates to coordinating V2G activity with the rest of the system generation/load, accounting for the grid topology, and identifying the appropriate control signals that ensure the beneficial behavior of numerous EVs.

In this direction, the Energy Planning Tool provides further insights into large-scale V2G deployment. As part of the SCALE Gothenburg pilot, i.e. a DN of the Chalmers University of Technology campus was studied across nine EV user charging scenarios. The analysis demonstrates the potential of systematic V2G integration under realistic mobility conditions and highlights the importance of combining detailed transport modelling, optimal siting of charging infrastructure, and continuous-time system simulation to ensure that widespread V2G adoption supports, rather than challenges, local grid operation.

—



1	DELIVERABLE ADMINISTRATIVE INFORMATION	1
2	PROJECT EXECUTIVE SUMMARY	2
3	SCALE PARTNERS	2
4	DELIVERABLE EXECUTIVE SUMMARY	4
5	LIST OF ABBREVIATIONS AND ACRONYMS	11
6	PURPOSE OF THE DELIVERABLE	12
7	BACKGROUND	13
8 GR	PART (A) EVS CHARGING STRATEGIES AND THEIR IMPACT ON A DISTRIBUTION	14
9	PART (A) FREQUENCY CONTROL ASSESSMENT WITH THE EV (V2G) SUPPORT	32
	PART (B): REPLICATION OF ENERGY PLANNING TOOL (T2.6) IN GOTHENBURG.OT	43
11	CONCLUSIONS	69
12	REFERENCES	70
13	ANNEX	72



List of figures

Figure 1: A schematic illustration of the V2G power flows	16
Figure 2: Hourly import and sell electricity prices for three days in June	19
Figure 3: Hourly electricity demand of the home for three days in June.	20
Figure 4: Optimised hourly electricity import/export of the home with discharge from EV for three days in June	21
Figure 5: Optimised hours and SoC of EV battery for three days in June.	21
Figure 6: Weekly average electricity imports and exports for the whole year2	22
Figure 7: Weekly average of discharge and spot price for the whole year2	22
Figure 8: Average of the three maximum monthly electricity imports for V1G and V2G2	23
Figure 9: Graph overviews of Grid 1. Green nodes indicate the homes while the grey ones are "empty"2	24
Figure 10: Graph overviews of Grid 2. Green nodes indicate the homes, while grey are "empty"2	25
Figure 11: Under-voltage problem in Grid 1: Voltage (upper) and power flow (bottom) results through the colormap for the selected hour and cases No-EV (left) and V2G (right)2	26
Figure 12: Over-voltage problem in Grid 1: Voltage (upper) and power flow (bottom) results through the colormap for the selected hour and cases No-EV (left) and V2G (right)2	27
Figure 13: Solved under-voltage problem in Grid 1 with PCC tap: Voltage (upper) and power flow (bottom) results through the colormap for the selected hour and cases No-EV (left) and V2G (right)2	
Figure 14: Solved over-voltage problem in Grid 1 with PCC tap: Voltage (upper) and power flow (bottom) results through the colormap for the selected hour and cases No-EV (left) and V2G (right)	30
Figure 15: Voltage values of the selected three nodes and time range in Grid 1: comparison between without (left) and with (right) the automatic PCC tap control and V2G case	31
Figure 16: The maximum and minimum values of voltage in Grid 2 over the whole year when no EVs are integrated and there are 10 PV panels	31
Figure 17: The maximum and minimum values of voltage in Grid 2 over the whole year when EVs (and PVs) are integrated in all homes with the V2G strategy	32
Figure 18: The scale analogy for frequency control and active power balance. In this project, hydro and EV's batteries are utilized.	33
Figure 19: The map of the NPS with the responsible TSOs. Only the East part of Denmark (the one belonging to the NPS – DK2) is illustrated. The figure is taken from (ref. 15,2023) and adjusted	34



Figure 20: The NPS test model: frequency responses and total FCR-D mechanical and electrical power deviations for the dimensioning disturbance without EV support.	
Figure 21: FCR-D ramp test of EV battery dynamic performance for different values of frequency contradelays	
Figure 22: FCR-D stability test of an EV frequency control model with the various frequency control de	
Figure 23: The NPS test model: frequency responses and total EVs power support for the dimensionin disturbance.	_
Figure 24: The impact of EVs regulating strengths increase on the system responses when zero EV frequency control delay is present.	41
Figure 25: Small-signal instability: the impact of EVs regulating strengths increase on the system responses when 0.5 s EV frequency control delay is present	41
Figure 26: Overall methodology of CERTH's Energy Planning Tool	45
Figure 27: Schematic representation of the current topology of the grid under study	46
Figure 28: Workplace charging scenario	47
Figure 29: Residential charging scenario	48
Figure 30: Public charging scenario	48
Figure 31: Fast charging scenario	49
Figure 32: Event charging scenario	49
Figure 33: Fleet charging scenario	50
Figure 34: Hotel charging scenario	50
Figure 35: University campus charging scenario	51
Figure 36: Weekend outing charging scenario	51
Figure 37: Grid Topology with installed charging stations for workplace charging scenario	54
Figure 38: Grid topology with installed charging stations in residential charging scenario	54
Figure 39: Grid topology with installed charging stations for public charging scenario	55
Figure 40: Grid topology with installed charging stations for fast charging scenario	56
Figure 41: Grid Topology with installed charging stations for event charging scenario	56
Figure 42: Grid topology with installed charging stations for Fleet charging scenario	57



Figure 43: Grid topology with charging stations for hotel charging scenario	58
Figure 44: Grid Topology with installed charging stations for university charging scenario	58
Figure 45: Grid Topology with charging stations for weekend outing charging scenario	59
Figure 46: State of charge for all scenarios from the chargers' point of view	60
Figure 47. Central Substation loading time-series.	62
Figure 48: Chalmers campus power system model for transport scenario 5	63
Figure 49: Requested and injected active power by V2G chargers for a. Scenario 1, b. Scenario 3 and Scenario 6	
Figure 50: Voltage magnitude evolution for a. Scenario 1, b. Scenario 3 and c. Scenario 6	67
Figure 51: Evolution of EV #1 battery state of charge and pack voltage in Scenario 1	68
List of tables	
Table 1: List of abbreviations and acronyms.	11
Table 2: Nomenclature and data relevant to MILP model applied to V2G.	15
Table 3: Parameters of the used model.	19
Table 4: Different costs compared with the reference case.	23
Table 5: Indication of voltage stability in Grid 1 for the whole year for different EV integration	28
Table 6: Improved voltage stability in Grid 1 for the whole year by using the PCC tap automatic control.	30
Table 7: Summary List of charging scenarios based on mobility pattern	52
Table 8: Position and nominal power of the chargers for workplace charging scenario	53
Table 9: Position and nominal power of the chargers for residential charging scenario	54
Table 10: Position and nominal power of the chargers for public charging scenario	55
Table 11: Position and nominal power of the chargers for fast charging scenario	55
Table 12: Position and nominal power of the chargers for event charging scenario	56
Table 13: Position and nominal nower of the chargers for fleet charging scenario	56



Table 14: Position and nominal power of the chargers for hotel charging scenario5
Table 15: Position and nominal power of the chargers for university campus charging scenario5
Table 16: Position and nominal power of the chargers for weekend outing charging scenario5
Table 17: Summary of optimal charging infrastructure location results6
Table 18: The list of synchronous generators in the NPS test model with the indication of bus number connection, name, active power output, the maximum active power out, base power, inertia constant, and indication if it is an FCR-D unit, respectively from left to right
Table 19: The list of wind power in the NPS test model with the indication of bus number connection, name, active power output, the maximum active power out, and base power
Table 20: HYGOV-TUR model parameters of the hydro FCR-D units in the NPS test model7
Table 21: The list of equivalent EV batteries in the NPS test model with the indication of bus number connection, name, active power output, and base power



5 List of abbreviations and acronyms

Table 1: List of abbreviations and acronyms.

Acronym	Meaning	
AC	Alternating current	
DC	Direct current	
dq0	Direct-Quadrature-Zero Transformation	
DN	Distribution Network	
DSO	Distribution System Operator	
ECM	Equivalent Circuit Model	
EV	Electric Vehicle	
EVCI	Electric Vehicle Charging Infrastructure	
FCR	Frequency Containment Reserve	
FFR	Fast Frequency Reserve	
LP	Linear Programming	
LV/MV	Low Voltage/ Medium Voltage	
MI(N)LP	Mixed-Integer (Non-)Linear Programming	
NPS	Nordic Power System	
PV	Photovoltaic	
RES	Renewable Energy Source	
SoC	State of Charge	
SSS	Small-Signal Stability	
TSO	Transmission System Operator	
V1G	Vehicle-one-Grid	
V2G	Vehicle-to-Grid	
WP	Work Package	



6 Purpose of the deliverable

This project introduces new system models, quantified results, and a detailed analysis of EV integration and its impact on the power system. It also explores how system operators can prepare for mass EV deployment. The key deliverables of this project are outlined below.

PART (A):

WP 5.2.1: Locally impacts on customers in residential areas, tariffs, optimization for use of V2G and V1G

- Models of two existing distribution grids, based on real grid topologies, cable data and end user data from smart meters.
- Studies and results of the impact on smart charging based of V1G vs V2G using a smart scheduling algorithm focusing on cost minimization (various grid tariffs included) for the customer without ancillary services.
- Studies and results relating **system loading and voltage issues** in distribution grid where V1G and V2G are being used based on smart (cost minimized) charging and discharging.
- Provides guidelines for avoiding voltage stability issues by identifying the grid's cable branches of concern and potentially mitigating the issue by using automatic voltage control at the PCC.

WP 5.2.2: Nordic Power System - frequency stability, technical requirements and delays considering decentralized or centralized V2G services

- **Frequency quality and stability evaluation** Analysis of the current state of frequency quality, including deviations beyond normal operating limits, and identification of major events that pose risks to frequency stability in the Nordic power system.
- **Fleet services** Investigation of the potential effects of V2G services on frequency stability, utilizing real-world data and large-scale power system simulations. The study considers the Nordic power system test model, projected reductions in system inertia, and future generation mixes up to at least 2040.
- **Study delays** Examination of delays in EV frequency control, battery capacity, and droop characteristics of governors and EVs. The study elaborates various dynamic responses of a large-scale Nordic power system test model and highlights important outcomes of the study.

PART (B):

Application of the Energy Planning Tool in Gothenburg pilot city

- Replication of the Energy Planning Tool, developed in T2.6, in a real-world MV DN at Chalmers University of Technology in Gothenburg.
- Development of nine EV charging scenarios reflecting diverse user behaviour, station types, and temporal patterns, used to evaluate system stress, scalability, and edge cases.



- Mobility-driven optimisation algorithm for siting EV chargers, minimising grid congestion and power losses without violating voltage or current limits, utilizing Pandapower (ref 1.) for the required power flow analysis and the Pymoo libraries (ref 2.) for meta-heuristic optimisation algorithms.
- Detailed V2G dynamic system models in Modelica language, simulating grid interactions with highfidelity representations of EV batteries, chargers, and the power grid.
- Scenario-based performance evaluation, including power flow calculations, setpoint tracking, SoC evolution, P/Q controller operation, and EV battery performance confirming the technical feasibility and control accuracy of V2G scheduling.
- Contribution to the scalability assessment of the tool under MV DN conditions, supporting future planning and DSO decision-making for large-scale V2G rollouts.

6.1 Attainment of the objectives and explanation of deviations

The objectives related to this deliverable have been achieved in full and as scheduled. There was a 2-month delay in the additional coordination between RISE and CERTH final deliveries.

6.2 Intended audience

The task 5.2 under WP5 focuses on simulation of mass deployment of V2G and evaluating the impact that V2G can have on the power system. The DSOs will benefit from understanding the impact on local levels in distribution grids by helping them make smart investments to create a more robust grid, while the TSOs will get an insight into the impact that V2G has on the stability of the larger power system. The project is also intended towards the aggregators who need to satisfy the technical requirements for frequency regulation to provide V2G services.

7 Background

The rapid expansion of Electric Vehicles (EVs) is reshaping the transport and energy sectors and playing a crucial role in decarbonization efforts. Governments worldwide have implemented ambitious policies to phase out internal combustion engine vehicles, promote EV adoption and accelerate the transition to a cleaner, more sustainable mobility system. The increasing availability of EV models, advances in battery technology, and falling costs have contributed to rising consumer adoption. As a result, global EV sales are growing at an unprecedented rate, and electrified transport is expected to become the norm in the coming decades. The electrification of transport is not only an environmental necessity, but also an economic and social transformation. By reducing dependence on fossil fuels, EVs help to reduce greenhouse gas emissions, improve urban air quality, and increase energy security by reducing dependence on imported oil. In addition, the shift to EVs has created new economic opportunities in industries such as battery manufacturing, energy management, and the development of charging infrastructure. However, this transition also poses challenges, particularly in the areas of electricity demand management and grid stability. The increasing penetration of EVs represents a new dynamic in electricity consumption, requiring innovative approaches to ensure that charging is done efficiently, flexibly, and in a way that supports rather than disrupts the electricity system.

On the other hand, the integration of EVs into the power system depends significantly on how and when they are charged. Uncoordinated or unmanaged charging, where vehicles charge as soon as they are plugged in, can exacerbate peak demand periods, increase grid congestion, and require costly upgrades to electricity infrastructure. To mitigate these issues, charging strategies must consider both grid constraints and economic signals. One of the most widely adopted solutions is controlled or smart charging, where charging schedules are optimized based on electricity prices, renewable energy availability, and grid conditions. By shifting demand to off-peak periods or aligning charging with renewable generation, smart



charging helps to balance supply and demand while lowering electricity costs for consumers. Beyond optimizing charging times, bidirectional charging technology introduces new possibilities by enabling EVs to discharge electricity back into homes or the grid. This approach, known as vehicle-to-home (V2G) and vehicle-to-grid (V2G), transforms EVs from passive energy consumers into active energy resources. By temporarily supplying electricity during peak demand hours or when electricity prices are high, EVs can help reduce peak loads, provide backup power to homes, and support overall grid stability. Bidirectional charging also allows EV owners to participate in energy arbitrage, storing electricity when prices are low and discharging it when prices are high, thus improving the economic value of EV ownership.

In addition to optimizing energy consumption patterns, EVs can play an important role in supporting the operation of the power grid by providing ancillary services. These services, traditionally provided by large power plants, ensure the stability and reliability of the grid. When aggregated and coordinated effectively, EVs can respond quickly to fluctuations in electricity demand and supply, helping to maintain system frequency, regulate voltage levels, and relieve grid congestion. The ability to discharge energy at specific times means that EVs can contribute to peak shaving by reducing electricity demand during critical hours, thereby improving overall grid resilience. The economic implications of using EVs to provide ancillary services are also significant. By participating in electricity markets, EV owners can generate additional revenue streams, further offsetting the cost of vehicle ownership. Aggregators and energy service providers are increasingly exploring business models that allow fleets of EVs to be collectively optimized for grid services, maximizing their value while minimizing the negative impact of battery degradation. As the energy transition accelerates, the role of EVs in grid flexibility is expected to become even more prominent, with advances in digital platforms, dynamic pricing models, and smart algorithms facilitating their seamless integration into electricity markets.

8 PART (A) EVs Charging Strategies and their Impact on a Distribution Grid

8.1 Smart home: electricity market aspects

Regulations and environmental targets, combined with rising energy costs and the reduction of fossil fuels, are posing global challenges. EVs play a crucial role in CO2 emissions in transition sectors. They can also provide benefits to owners and society, for example, by charging in demand response mode to maintain grid stability and peak shaving purposes (ref. 3, 2023). This interaction between EVs, the grid, and the home can be achieved through unidirectional smart charging (V1G or V1G) and bi-directional charging/discharging, which, unlike V1G, also allows the EV battery to be discharged to the grid or the home during periods of high electricity prices or demand. This technology, Vehicle to Grid (V2G), is growing rapidly due to the accelerated electrification of the transition sector, together with the increase in variable renewable generation, which poses a challenge to the stability of the electricity grid (ref. 4, 2022). A smart EV charging schedule can minimize the impact of EVs on grid stability. V2G can also be considered as an opportunity to generate incentives and profits for the owner by enabling bi-directional charging. Several studies have investigated the economic benefits of V2G. Study (ref. 5, 2017) evaluated the economic benefits of V2G for a detached house with different heating sources using a Mixed-Integer Linear Programming (MILP) model, real EV charging data, and day-ahead hourly electricity prices. The results showed that V2G could save about 11% of the total annual electricity costs. They also evaluated the explicit EV demand response model. The economic benefits of smart charging, a V2G, and space thermal load control of a PV-connected house are investigated using Linear Programming (LP). The V2G model showed higher annual cost savings (12-20%) than the space thermal load control case for 1-10 houses with different EVs. Also, the additional cost savings of V2G compared to the V1G are limited (less



than 1%) due to battery degradation costs. In the study in (ref. 6, 2022), a household with PV and bidirectional EV charging was optimized using both LP (with fixed battery efficiencies) and MILP (with nonlinear battery efficiencies) models. The non-linear charging and discharging efficiencies of the EV battery in the MILP model give a more realistic profit (30% lower than in LP). The profit is about 310€ per year, mainly obtained in summer.

EV participation has also been studied in ancillary service markets. An optimization model for V2G has been developed for the Frequency Containment Reserve (FCR) market, taking into account battery degradation (ref. 7, 2023). The profit that an EV can make by participating in the FCR market was investigated using a MILP model. The results showed that participation in the FCR market is quite profitable for the EV owner. In (ref. 8, 2021), a stochastic optimization method was proposed to investigate the optimal FCR profile while maximizing the potential profit of EV charging station participation in the day-ahead market. The results showed that FCR for normal disturbances (FCR-N) leads to higher profit than FCR for large disturbances (FCR-D) due to the difficulty of charging stations to provide a down-regulation reserve. The most optimal choice is a combination of FCR-D and FCR-N products for charging stations; however, providing FCR-D is more practical as it has less impact on EV owners' preferences.

This section presents the charging schedule of bidirectional V2G for a household with photovoltaic (PV), taking into account the estimation of electricity tariff costs. A MILP model has been used with real EV charging data to investigate hourly driving energy consumption. Hourly driving energy consumption is available, hourly electricity demand of the house and hourly electricity prices are used as inputs in the model. The model minimizes the electricity costs of an EV and a house. The insights are then reported through twenty V2G models comprising different driving pattern data and home demand to see the pattern of variables during the year. In addition, the model is used to compare two cases where two charging strategies are considered: a bi-directional V2G case and a V1G or demand response case where the charging schedule is minimized by applying a 'smart charging' strategy. This is also referred to as implicit demand response, where charging is scheduled during the cheaper hours or when demand is lower (ref. 3, 2023).

8.2 Mixed-Integer Linear Programming (MILP) model

In the following, the fundamentals of MILP model applied in the V2G optimization are explained. To follow the technical context of the section, the appropriate nomenclature is given in Table 2.

Table 2: Nomenclature and data relevant to MILP model applied to V2G.

Description/Name	Variable	Unit
Load data	E_t^{dem}	kWh
Solar production data	E_t^{pv}	kWh
Electricity and grid costs	c_t^{el} , c_t^{grid}	SEK/kWh
Sell cost	\mathcal{C}_t^{sell}	SEK/kWh
Battery energy capacity	$E_{max,b}$	kWh
AC/DC and DC/AC invertor efficiencies	η_{ac_dc} , η_{dc_ac}	/



Battery charge and discharge efficiencies	$\eta_{charge}, \eta_{disc}$	/
Import and export electricity	E_t^{im},E_t^{ex}	kWh
Charge from PV to EV	E_t^{pv-ev}	kWh
Charge from grid to EV	E_t^{g-ev}	kWh
Discharge of the battery to house	E_t^{g-h}	kWh
State of charge of the battery	E_t^{SoC}	kWh
The largest peak of imported electricity per optimization period T	E_{lim}	kWh
Power tariff (peak power) cost	p_{tariff}	SEK/kWh
Electricity consumption for transportation	$E_t^{driving}$	kWh
Cost to penalize the peak power related to the electricity imported	C _{power}	SEK/kWh

A schematic of the V2G system is shown in Figure 1. The model aims to minimize the total electricity cost for the owner of the EV connected to the house. Figure 1 shows the bi-directional charging of the EV to the house with solar PV production. The aim is to minimize the cost of electricity purchased from the grid for the house and the EV and to maximize the electricity sold to the grid during periods of low demand or high prices.

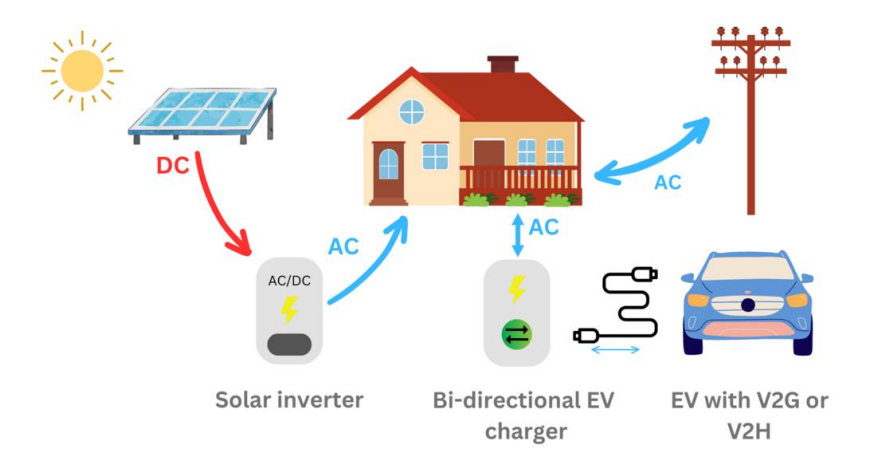


Figure 1: A schematic illustration of the V2G power flows.



The mathematical formulation of the optimisation model is described below. The objective function minimises the total electricity cost over the year. It includes for $t \in T$ the total optimisation time.

$$\min \sum_{t}^{T} E_{t}^{im} \left(c_{t}^{el} + c_{t}^{grid} \right) + c_{power} - E_{t}^{ex} c_{t}^{sell}, t \in T$$

$$\tag{1}$$

Where P_t^{im} and P_t^{ex} is the power imported (bought) and exported (sold) to the household in kW. c_t^{el} is the cost of electricity, which varies over time according to the spot market, and c_t^{grid} is the grid fee, which may vary over time, but in this case is constant over time. The c_t^{sell} is the cost the household receives for selling electricity to the grid. c_{power} is the cost to penalize the peak power related to the electricity imported and is defined as:

$$c_{power} = max\{E_t^{im} p_{tariff}\}, \qquad t \in T$$
 (2)

Where the maximum expression indicates the average of the three largest peaks of purchased electricity within the time period t, in kWh/h. The power tariff (p_{tariff}) or power peak cost is the cost to penalise the largest peaks of electricity purchased in SEK/kW. In this analysis, it is the average of three largest peaks of imported electricity for each month of the year that defines the electricity cost.

The optimisation model is solved for one year with a rolling horizon, with an optimisation horizon of 24 hours, T, and a horizon of 12 hours. Thus, each time period, T, is optimally solved as an individual entity until the sum of these time periods equals the entire time period under consideration, one year. This means that for each iteration of the optimisation, the input data consists of 24 hours of demand, PV production and prices. In each optimisation, the solution data for the first twelve hours of the period are stored. The remaining hours are run through the model again for the next time period t, as the time step is 12 hours.

The constraints of the model include constraints from (3) to (11). In the energy balance constraint, electricity consumption is equal to electricity production:

$$E_t^{im} + E_t^{pv} + E_t^{disc} = E_t^{ex} + E_t^{dem} + E_t^{pv-ev} + E_t^{g-ev}$$
(3)

State of charge for battery is calculated in equation (4) in which the driving load of the EV is deducted from E_t^{SoC} in each time step.

$$E_t^{SoC} = E_{t-1}^{SoC} - \frac{E_t^{disc}}{\eta_{disch}} + \eta_{charge} \left(E_t^{pv-ev} + E_t^{g-ev} \right) - E_t^{driving}$$

$$\tag{4}$$

Boundary conditions are introduced from (5) to (10). Constraints (5) to (8) set the boundary conditions for electricity export, charge, discharge, and state of charge of the battery.

$$E_t^{ex} \le \eta_{dc/ac} E_t^{pv} + E_t^{disc} \tag{5}$$

$$E_t^{pv-ev} + E_t^{g-ev} \le 0.8 E_{max,b}$$
 (6)

$$E_t^{disc} \le E_t^{disc,max} \tag{7}$$

$$E_t^{pv-ev} + E_t^{g-ev} \le \alpha_t (E_t^{SoC} - E_{t-1}^{SoC} + E_t^{disc})$$
 (8)

WWW.SCALE.EU _______ 17



A binary parameter α_t is considered to determine the availability of the car at home. Corresponding to the available data from the car travelling, when the car is at home, it is 1, and when the car is travelling, it is considered as 0. Constraints (8) and (9) set the charging and discharging of the battery to zero when $\alpha_t = 0$, or to a non-zero value when $\alpha_t = 0$ in each hour.

$$E_t^{disc} \le \alpha_t E_t^{SoC}$$
, binary parameter : $\alpha_t = \{0,1\}$ (9)

Finally, we need to ensure that the EV has at least 80% of its capacity charged before the departure time, meaning that the following is valid:

when
$$\alpha_{t-1} = 1$$
 and $\alpha_t = 0$, then it must be that $E_t^{SoC} \ge 0.8 E_{max,b}$. (10)



8.3 Test model of a home

8.3.1 Input data

In this part, the input data used to simulate in the model and output are introduced. Time series used in the model as inputs are hourly PV production, home demand and spot prices. In addition, there are hourly consumption data for car travel. Table 3 presents different data used in the model. Constant parameters are used for the battery and solar DC-AC inverter. The efficiency for AC inverter has been considered as 1. Table 4 presents the parameters.

Table 3: Parameters of the used model.

η_{dc-ac}	η_{ac-dc}	η_{charge}	η_{disch}	$E_{max,b}$ (kWh)	$P_{max,dis}$ (kW)
0.985	1	1 0.975 0.9		50	11

It is assumed the charging point has not a limited rate. The discharge of battery can be maximum 11 KW in each hour, but to consider the highest possible benefit from EV, charging in each hour is possible to full capacity. Figure 2 shows the calculated electricity import and sell prices in the model for three days in June, between 4-7 June 2019. Network price, electricity certificate, tariff are the parameters used to compute the prices. The load data of the home also his shown in Figure 3 for three days.



Figure 2: Hourly import and sell electricity prices for three days in June.



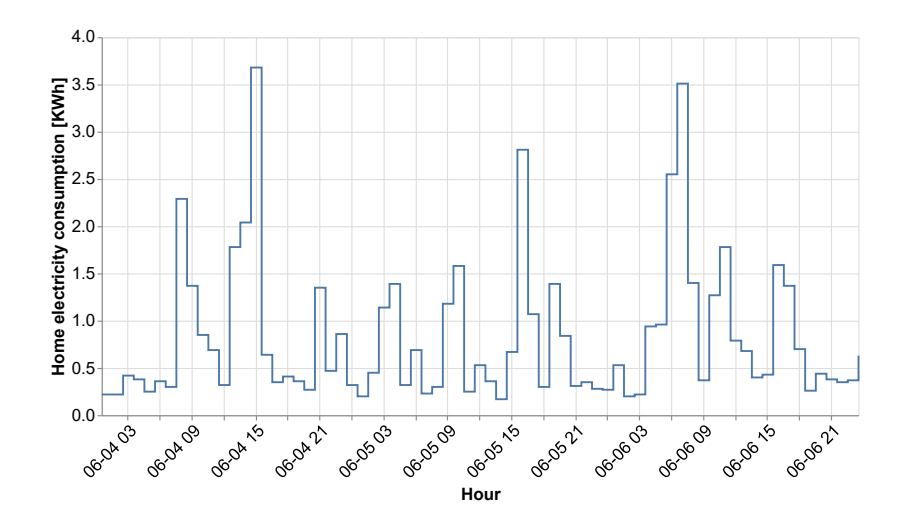


Figure 3: Hourly electricity demand of the home for three days in June.

The decision variables are hourly electricity import and export costs and the operation of the battery. Objective function determines the total yearly cost.

8.3.2 Results

The electricity imports and exports and the battery operation of the EV are presented as model results. In the first part, we analyse the results of only one V2G unit. In the second part, we have modelled 20 homes and present the weekly average of the optimised variables for the EVs. Finally, the two case studies are considered; the V2G and V1G (smart charging without discharge) cases.

Note: The appropriate terminology in this section would be Vehicle-to-Home (V2H) and Vehicle-1-Home (V1H), but to keep the same terminology throughout the report, V2G and V1G are used instead.

8.3.2.1 One V2G model

Figure 4 shows the hourly electricity import and export, total PV production and discharge from EV for three days in June starting from 12:00. June was chosen because of higher PV production. Most of the electricity exports are covered by PV production and for some hours by discharge from EV, depending on the availability of the car. This happens whenever there is high PV production around midday, or sometimes during lower household demand, as shown in Figure 2 and Figure 3. During hours of higher demand, the demand is met either by discharging the EV when the car is available at home, or by importing electricity when the car is not at home.



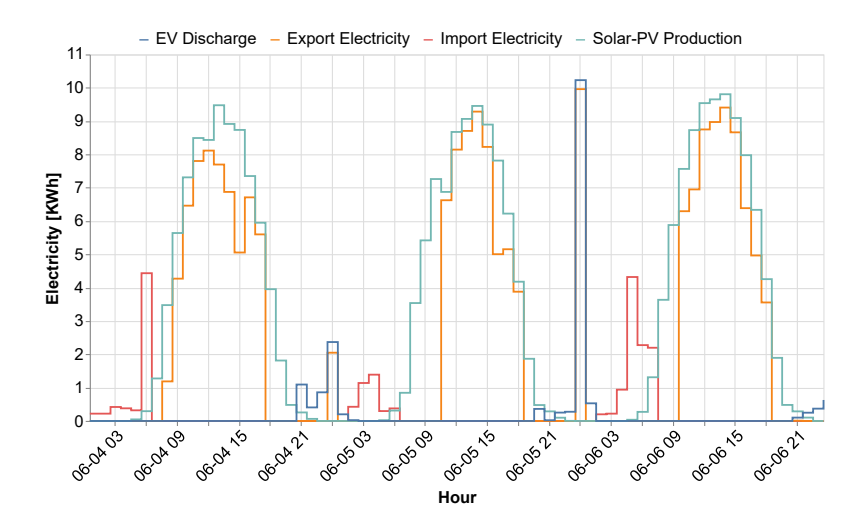


Figure 4: Optimised hourly electricity import/export of the home with discharge from EV for three days in June.

Figure 5 shows the operation of the battery, including the hourly charging of the battery from the grid and PV, the discharge from the EV to the home, and the SoC of the battery on the secondary axis. Charging the battery from the grid occurs mainly when electricity prices are low. At higher prices, the remainder of the PV production after export goes to the battery in the morning before the car's departure time. Discharge, also shown in Figure 5, occurs when the price or demand is high. The SoC includes the hourly driving energy consumption. It increases as the car is charged at night and decreases during the day when the car is travelling.

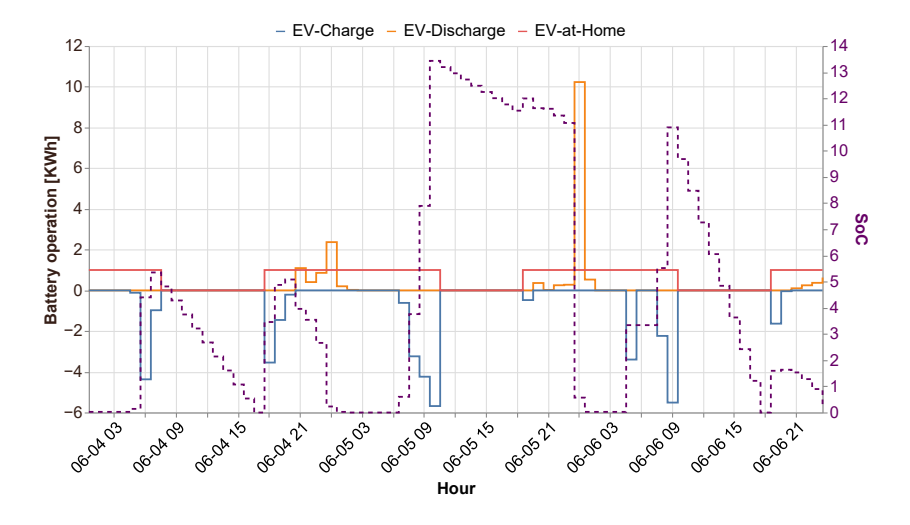


Figure 5: Optimised hours and SoC of EV battery for three days in June.

8.3.2.2 Twenty V2G models

The higher resolution shows a better pattern of variables in the results. The model was used to simulate 19 different V2G systems using 19 different load and trip data. Figure 6 and Figure 7 show the weekly average of the variable, electricity import and export and discharge. The spot price as an input parameter has also been shown to compare and evaluate its impact on the



results. Based on Figure 6, export and import are inversely proportional. Weekly fluctuations can be observed, as well as a certain correlation between falling export and rising import.

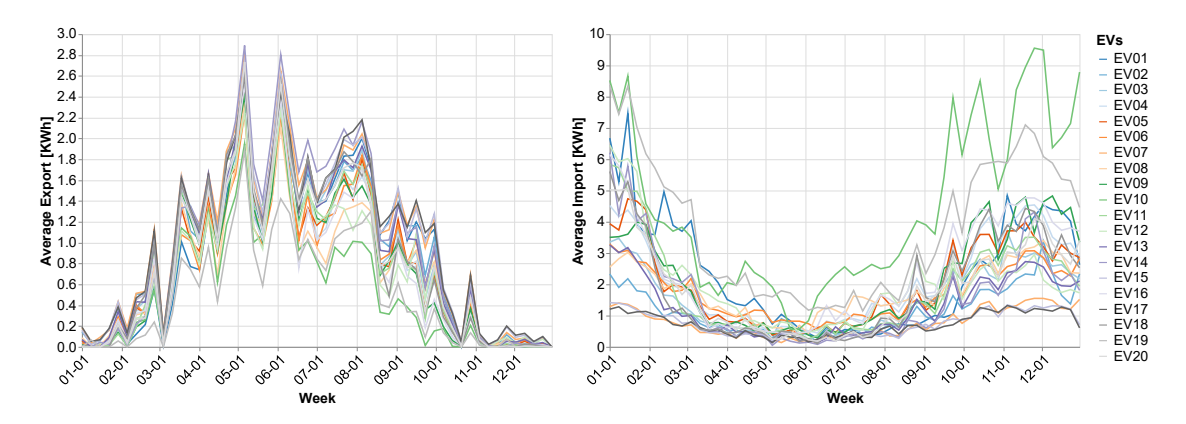


Figure 6: Weekly average electricity imports and exports for the whole year.

Figure 7 shows weekly averages of outflows and spot prices. The presentation of weekly averages over the year shows that the model continues to capture the long-term price variations observed in the charts. In particular, the results clearly show higher offtake in the peak period of the spot price and a lower offtake in the off-peak period of the price.

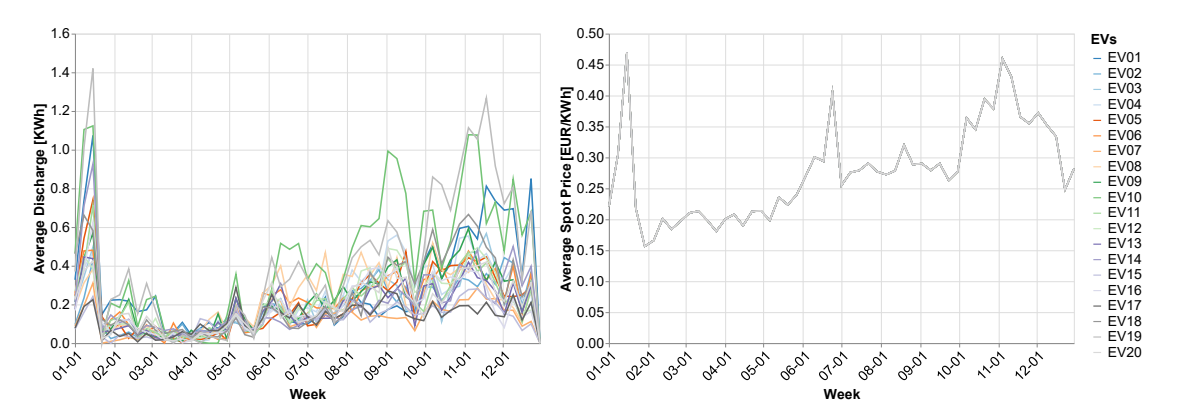


Figure 7: Weekly average of discharge and spot price for the whole year.

8.3.2.3 Comparison between V2G and V1G cases

The impact of the cases on the household's total annual costs is shown in Table 4. The lowest annual cost is related to the V2G case. The bidirectional V2G model is discussed in the previous section. On the other hand, the V1G case is optimised to take advantage of the low electricity price during low demand, without discharging at home. The driving costs of the EV cases are excluded from the total annual costs; however, the electricity consumption for driving is considered. The annual cost in V2G case is high because the car is connected to the home



based on availability and cannot discharge to the grid as the role of a stationary battery. However, V1G case is slightly higher than V2G, but it is not significant in this model.

Table 4: Different costs compared with the reference case.

Case	Total yearly cost (kSEK)	Power peak cost (kSEK)	Maximum monthly power peak (KWh)
V2G	22.96	2.27	17.62
V1G	23.67	2.49	17.83

The annual peak power cost in the bidirectional V2G case is 8.7% lower than in the V1G case. In this model, the electricity tariff is based on the average of the three highest monthly peaks. Costs could be higher if the tariff were calculated from the highest daily electricity import.

Figure 8 shows the distribution of these monthly power peaks, highlighting how V2G reduces peak demand every month by allowing energy to be discharged and stored.

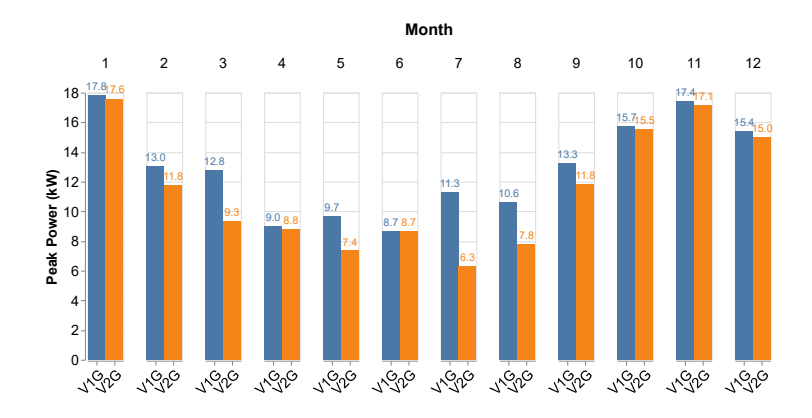


Figure 8: Average of the three maximum monthly electricity imports for V1G and V2G.

Unlike V1G, where the vehicle can only charge, V2G can supply energy to the household or grid, flattening the demand curve. By selling energy during high-price periods, V2G offsets purchases, resulting in a more balanced consumption profile and lower net energy peaks. This reduces reliance on grid imports during critical hours, lowering peak energy costs and making V2G a more cost-effective and grid-friendly solution. The benefit of V2G may change with different data. Battery characteristics such as discharge/charge capacity and efficiencies have a large impact on the results.

8.4 Test system models of distribution grids

When a new unit—such as a home, a Renewable Energy Sources (RES), or an EV—is connected to the grid, it is crucial to consider its impact on voltage levels and cable loadings throughout the distribution network. Traditionally, distribution grids have a radial structure with no embedded generation. As a result, power flow was unidirectional, and the primary challenge was managing undervoltage issues at the grid's extremities.

WWW.SCALE.EU _______ 23



However, the introduction of RES has changed this dynamic, making over-voltage a significant concern. The integration of EVs, each with different control strategies, has further complicated voltage stability, introducing both opportunities and risks.

In the following subsections, the integration of PV-EV units into residential homes is examined and evaluated within two realistic distribution grids. The analysis considers the EV charging methodologies outlined in previous sections, along with annual loading profiles.

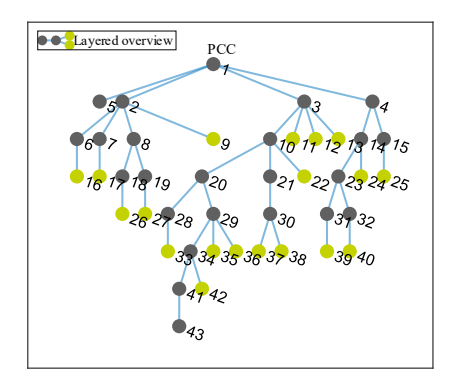
The low-voltage distribution grids under investigation are:

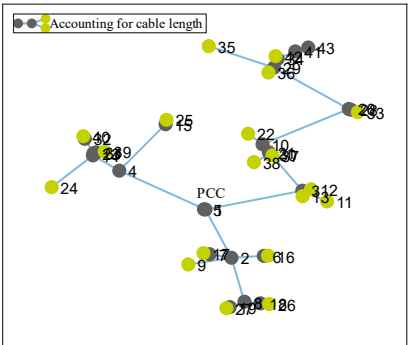
- Network Station LBG A rural network with a nominal voltage of 400 V, consisting of 43 nodes and 19 homes.
- **Borås Electricity Network** A network with a nominal voltage of 400 V, comprising 72 nodes and 57 homes.

The applied cable properties are based on real-world data, while household consumption patterns are derived from actual loading data from year 2019 for Grid 1, and 2018 for Grid 2. PV production is integrated into all homes on top of the baseline consumption from historical data. A single PV has a capacity of 13.7 kW, and its profile follows a typical PV activity throughout the year, while a single EV power capacity is 11 kW, and these values are applied for all test cases.

Figure 9 and Figure 10 depict the graphical representations of both grids, illustrating three different visualization methods. The layered representation provides a structured view, showing how nodes are arranged hierarchically. In contrast, the graphs that account for realistic cable lengths and electrical distances offer better insight into which nodes might become voltage-critical under heavy loads. In this context, electrical distance refers to the actual cable resistance, calculated as the resistance per unit length multiplied by the cable's actual length.

In all diagrams, the nodes representing homes are highlighted in green, while empty nodes are shown in grey. The Point of Common Connection (PCC) to the medium voltage grid is also shown.





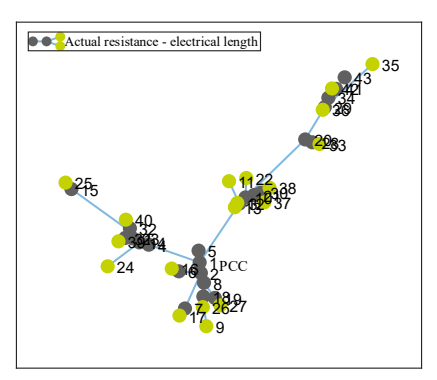
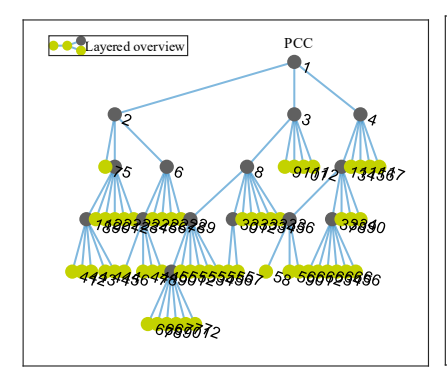
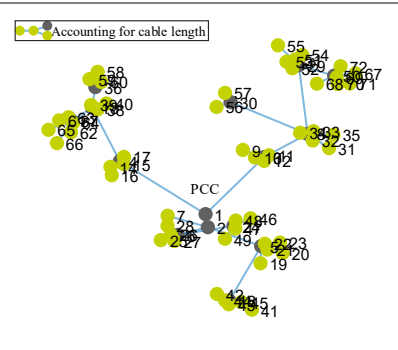


Figure 9: Graph overviews of Grid 1. Green nodes indicate the homes while the grey ones are "empty".

WWW.SCALE.EU ______ 24







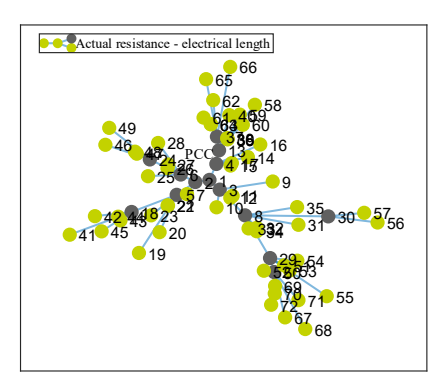


Figure 10: Graph overviews of Grid 2. Green nodes indicate the homes, while grey are "empty".

It is important to note that a node appearing "far away" in the single-line diagram does not necessarily mean its actual electrical distance is equally significant. Additionally, longer cables may have lower total resistance if they have a larger cross-section, as this reduces their per-unit resistance.

8.5 EVs charging impact on the two cases distribution grids

Accounting for the results obtained in Section 8.3, and by running the power flow for the whole year using the Newton-Raphson method, one can obtain the voltage values across the grid for the following cases:

- No-EV: Home consumption accounts for PV integration but without EVs,
- V1G: Home consumption accounts for both PV and EV with V1G charging strategy,
- V2G: Home consumption accounts for both PV and EV with V2G charging strategy.

To understand the fundamental impact of EV integration, two interesting scenarios are presented for the chosen hours for Grid 1, where voltage profile and grid loading are depicted in the grid's graph.

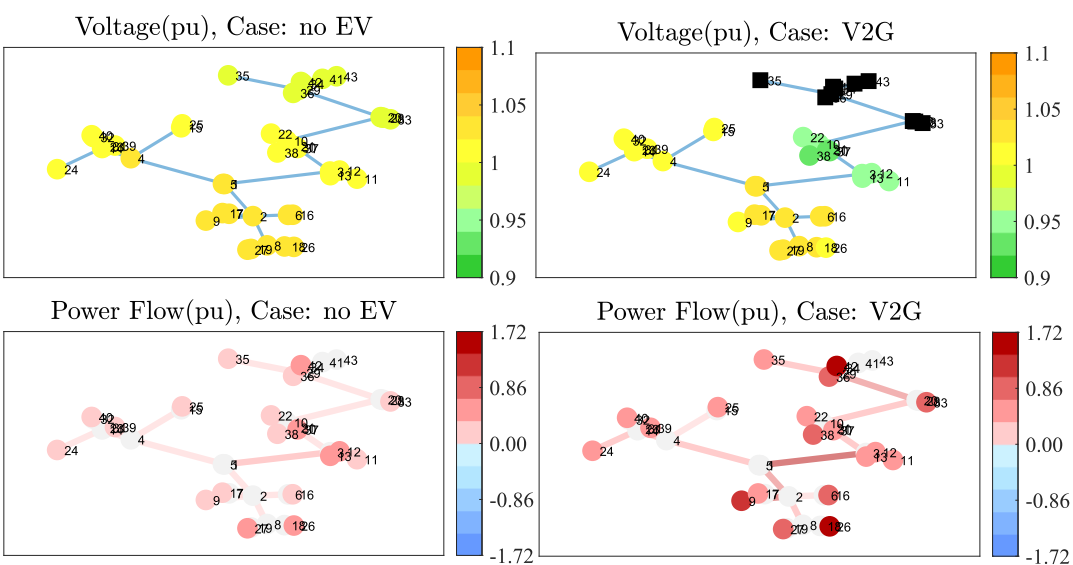
8.5.1 Under-voltage problem in Grid 1 for the selected hour

Figure 11 shows the difference between the results of power flow in cases between No-EV (left figures) and V2G (right figures). The upper figures show the results of voltage values, and the bottom ones show the results of nodes and line loading (also highlighting the power flow directions). The per unit value of power flow is scaled based on the values in the No-EV case so that it can be seen how these values change with EV integration.

Note: The scaling in the figures below is done separately for each node and line. Node or line i in case of V2G is scaled for the largest value of power of node or line i in the No-EV case.

WWW.SCALE.EU _______ 25





Grid 1: Under-Voltage Problem illustrated for: 23-Mar-2018 03:00:00

Figure 11: Under-voltage problem in Grid 1: Voltage (upper) and power flow (bottom) results through the colormap for

Figure 11 portrays how, in the middle of the night, there is generally low loading across the grid in the No-EV case, and there are no voltage issues. However, once V2G is implemented, accounting for the charging strategy shows that several nodes are heavily loaded, and the voltages in that area end up being below the allowed margin - there is an under-voltage instability (on black nodes). This effect can also be seen with V1G since it includes nighttime charging. The color of the cables in V2G case is dominantly red since most

8.5.2 Over-voltage problem in Grid 1 for the selected hour

the selected hour and cases No-EV (left) and V2G (right).

of the homes are taking electricity from the grid.

Similarly to the previous case, the results in Figure 12 are now shown for the hour of high PV integration, which causes an over-voltage problem in the No-EV case (black nodes). However, with EV integration, and the V2G charging, the voltages are only slightly improved and do not remain within the acceptable margin.



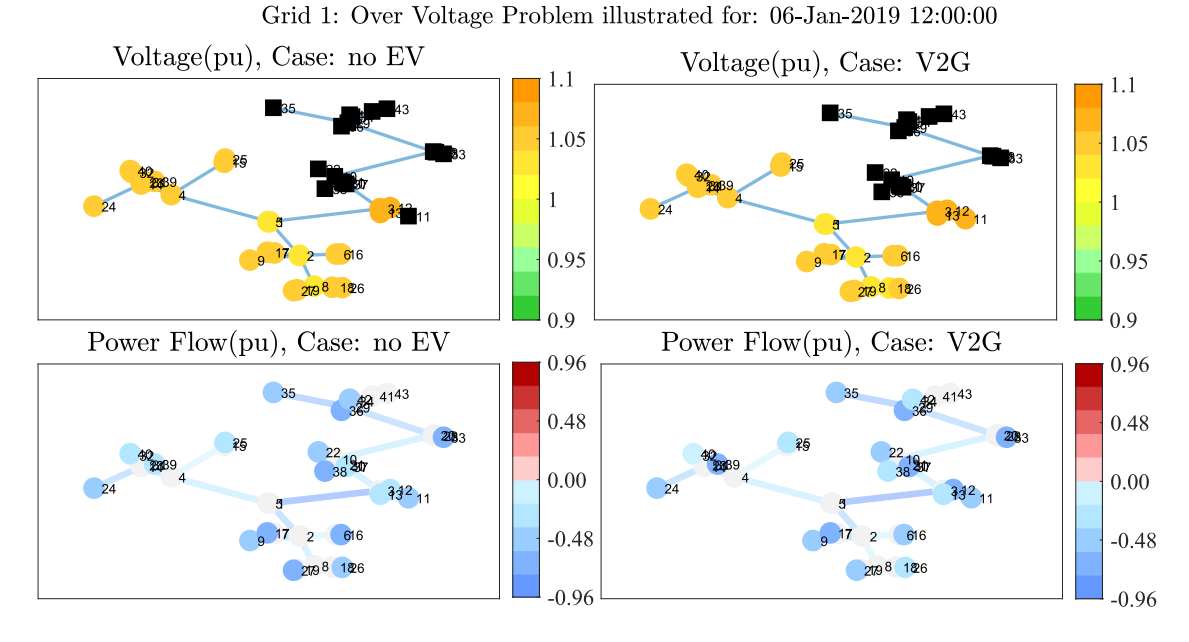


Figure 12: Over-voltage problem in Grid 1: Voltage (upper) and power flow (bottom) results through the colormap for the selected hour and cases No-EV (left) and V2G (right).

The main message is to consider carefully the size of the EV-PV integration with respect to the grid configuration. These types of grid issues cannot be neglected and ideally should be integrated in electricity market algorithms.

8.5.3 Voltage stability characterization over the whole year: Grid 1 results

The above results relate to the specific hours and show the results for all the nodes in the grid. However, additional metrics are needed to quantify the voltage stability or performance over the whole grid. In this case, we define three that characterize the grid's voltage stability:

- The number of over-voltage instabilities per node over the whole year
- The number of over-voltage instabilities per node over the whole year
- The specific robust voltage-stability parameter $v_{stab,qrid}$ for the whole year is defined in the following way:

$$v_{stab,grid} = \sum_{i=1}^{n_{nodes}} \sum_{t=1}^{8760} c_{vs,t}^{i}$$
, where (11)

$$c_{vs,t}^{i} = \left(\frac{|V_t^{i} - (1 \pm \Delta V_{rm})|}{\Delta V_{rm}}\right)^{n_{penalty}},\tag{12}$$

and $c_{vs.t}^i$ is nonzero only if:

- $\begin{array}{ll} \circ & V_t^i > 1 + \Delta V_{rm} \text{ pu with the "+" sign, or} \\ \circ & V_t^i < 1 \Delta V_{rm} \text{ pu with the "-" sign,} \end{array}$

where all the voltages are in pu, the robust margin is $\Delta V_{rm} = 0.05$ pu, $n_{venalty} = 3$, and n_{nodes} represents the total number of nodes in the grid.



Parameter $c_{vs,t}^i$ is arbitrarily made and serves to penalize the nodes where voltage deviations are $5\% = \Delta V_{rm}$ higher than the nominal value. If they are below, then it is considered that no penalization is needed. Parameter $n_{penalty} = 3 > 1$ is introduced to penalize stricter the voltage deviations higher than 10% (which is the maximum allowed margin for the system to be considered as voltage stable).

1113

1172

1 098

1.201

For the three scenarios of EV integration and charging strategy in Grid 1, the three parameters that were obtained are listed in Table 5.

Case	Total under- voltage instability	Total over-voltage instability	$v_{stab,grid}$
No-EV	0	1252	1.292

45

176

V₁G

V2G

Table 5: Indication of voltage stability in Grid 1 for the whole year for different EV integration.

Table 5 shows that large PV integration provides a huge (over-voltage) problem for the grid, and therefore, it will be unfeasible to integrate such a large amount of PV. The integration of EVs only marginally has a positive impact on voltage stability, which can be seen in the reduced value of the over-voltage instances. However, there is an increased number of under-voltage instability events. Interestingly, for the given grid and cases, V1G is more beneficial for grid stability than V2G.

8.5.4 A measure to improve voltage stability in distribution grids: Grid 1 results

There are several approaches to enhancing voltage stability in a distribution grid, particularly when addressing the challenges of PV integration—an issue that has been a major concern even before the integration of EVs. If grid operators are willing to invest, a straightforward solution is to reinforce the radial sections by adding more cables where voltage and loading issues arise or to transition the grid from a radial to a meshed structure by introducing additional connections.

However, if expanding the cable network is not a viable option, voltage stability can be improved by adjusting the PCC voltage values. Traditionally, the PCC voltage was set to 1.05 pu by default, which may not be suitable for large-scale PV integration. A simple alternative is to determine a more optimal fixed value and adjust it manually on a seasonal basis. However, the rapid fluctuations in RES—such as PV power output and EV charging or discharging—occur on much shorter time scales than seasonal changes, making this approach less effective.

A more adaptive solution is to implement an automatic tap changer at the PCC bus transformer. In this project, the proposed approach is for the automatic tap to adjust based on the real-time loading conditions of the downstream cables. This means that when cable loading increases, the PCC voltage can be raised, while high PV generation would usually imply a reduction in PCC voltage. This strategy has been implemented in Grid 1, with the results presented below.

The recommended PCC voltage control is defined as follows:



$$V_{PCC,t,rec} = V_{L0} + \frac{V_{max} - V_{min}}{P_{ds,max} - P_{ds,min}} P_{ds,t}, \text{ where}$$

$$\tag{13}$$

$$P_{ds,t} = \sum_{i=1}^{n_{ds}} P_{ds,t}^{i},\tag{14}$$

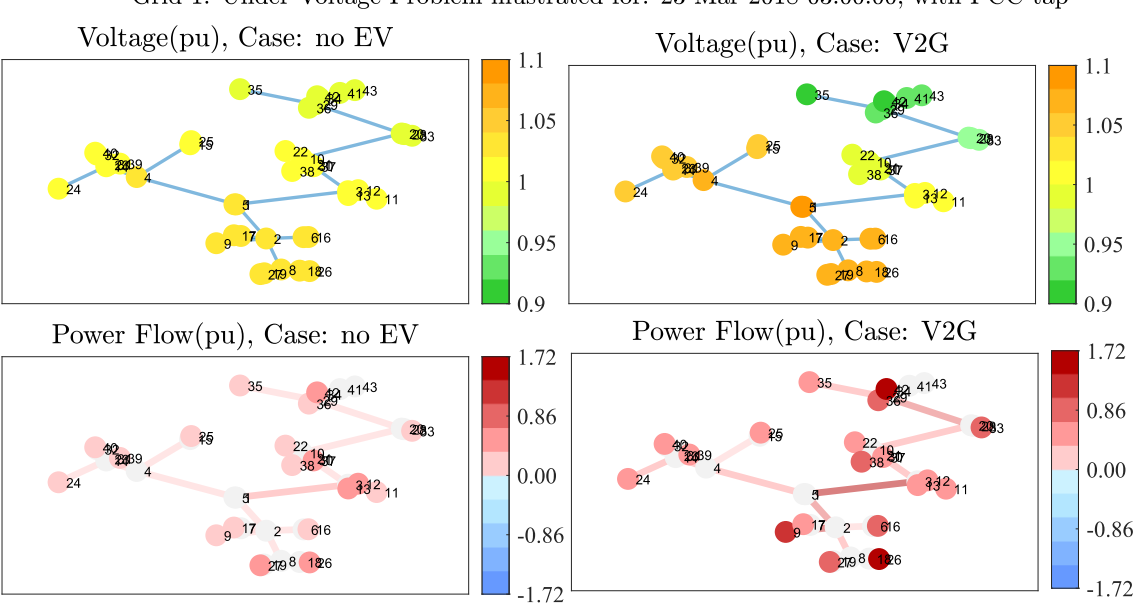
and $P_{ds,t}^i$ represents active power loading at the hour t of a downstream cable i of a critical radial stream that has a voltage stability problem. The maximum and minimum allowed voltages are $V_{max}=1.1$ pu and $V_{min}=0.9$ pu. $P_{ds,max}=0.05$ pu and $P_{ds,min}=-0.1$ pu represent the approximate maximum and minimum values of $P_{ds,t}$ over the year in the No-EV case. $V_{L0}=1.01$ pu is a no-load voltage, and it is an optimization product that reduces the number of total over- and under-voltage instabilities over the year.

The recommended PCC voltage $V_{PCC,t,rec}$ is equal to the actual PCC voltage $V_{PCC,t}$ only if the following is fulfilled:

- $V_{PCC,t,rec}$ is within the limits of $[V_{min},V_{max}]$, otherwise it is saturated within that range.
- The amplitude of the voltage step from t 1 to t is not higher than 0.02 pu when V_{PCC,t,rec} is within [0.94, 1.06] pu, otherwise the voltage step is limited to 0.02 pu.
 Remark: Further restrictions to limit the tap number over the year and avoid stressing the

transformer are possible. This is one illustrative example. A grid operator decides which voltage control type is the most suitable, considering the grid configuration and load/PV/EV behavior.

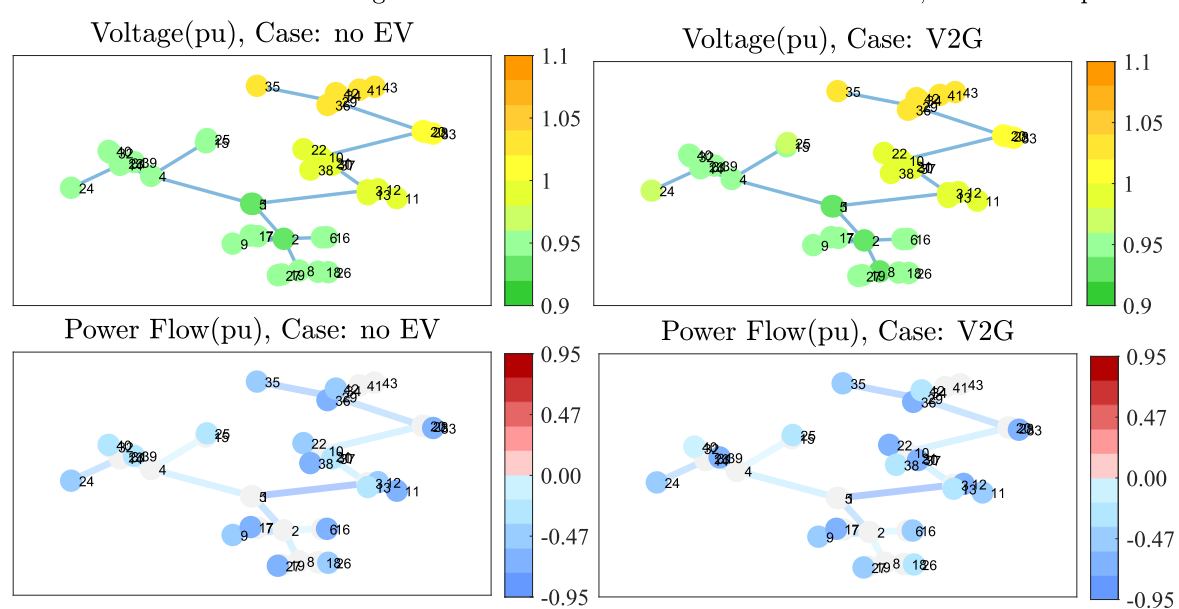
The results of such automatic PCC tap control show the following improvements in Grid 1 voltage stability in Figure 13, Figure 14, and Table 6, which are dual to results when no tap PCC control is applied in Figure 11, Figure 12, and Table 5, respectively.



Grid 1: Under-Voltage Problem illustrated for: 23-Mar-2018 03:00:00, with PCC tap

Figure 13: Solved under-voltage problem in Grid 1 with PCC tap: Voltage (upper) and power flow (bottom) results through the colormap for the selected hour and cases No-EV (left) and V2G (right).





Grid 1: Over-Voltage Problem illustrated for: 06-Jan-2019 12:00:00, with PCC tap

Figure 14: Solved over-voltage problem in Grid 1 with PCC tap: Voltage (upper) and power flow (bottom) results through the colormap for the selected hour and cases No-EV (left) and V2G (right).

Table 6: Improved voltage stability in Grid 1 for the whole year by using the PCC tap automatic control.

Case	Total under- voltage instability	Total over-voltage instability	$v_{stab,grid}$
No-EV	0	0	0
V1G	0	0	0
V2G	0.027	0.042	0.085

Figure 13 and Figure 14 illustrate how the PCC voltage adjusts to the loading of the critical radial downstream and helps their voltages to remain within the allowed voltage margin.

To confirm how PCC voltage control impacts positively the values of the two voltages at nodes 24 and 35 at the "ends of the grid", Figure shows the time range between 2200 and 2350 hours for the V2G case.



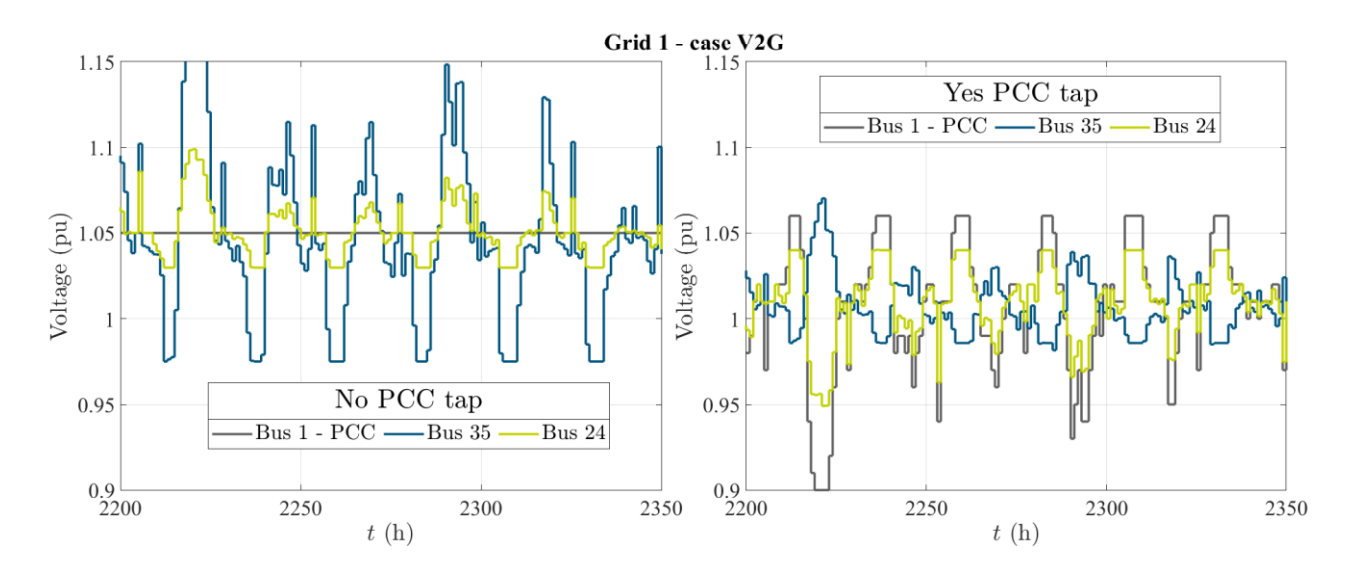


Figure 15: Voltage values of the selected three nodes and time range in Grid 1: comparison between without (left) and with (right) the automatic PCC tap control and V2G case.

8.5.5 Voltage stability in Grid 2

The following analysis pertains to the Grid 2 test case. This model includes more homes but maintains a similar radial grid structure. The initial test focuses on PV integration alongside household load consumption, without the presence of EVs.

Unlike in Grid 1, where PV integration was more manageable, running power flow simulations with all 57 homes equipped with 13.7 kW PV panels results in significant overvoltage stability issues. Even with only 10 homes having PV panels, voltage violations occur frequently. Figure 16 illustrates the maximum and minimum voltage levels, highlighting recurring instances where maximum voltage exceeds the permissible limits.

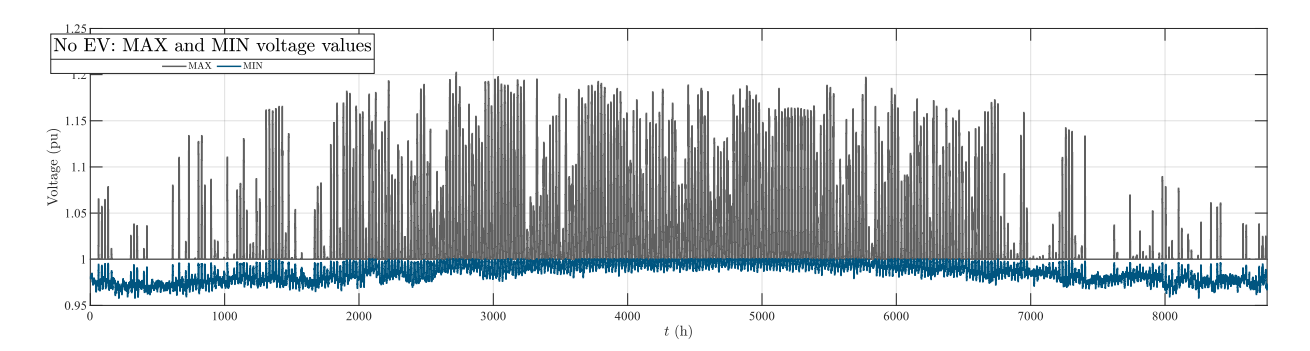


Figure 16: The maximum and minimum values of voltage in Grid 2 over the whole year when no EVs are integrated and there are 10 PV panels.

In the next case, both PV and EV integration are implemented across all 57 homes. Figure 17 presents the maximum and minimum voltage levels in the grid throughout the year for the V2G EV implementation.

The results indicate that PV and EV complement each other effectively, preventing voltage limit violations without requiring additional PCC voltage control or other corrective measures. Similar results are observed for the V1G charging strategy as well.



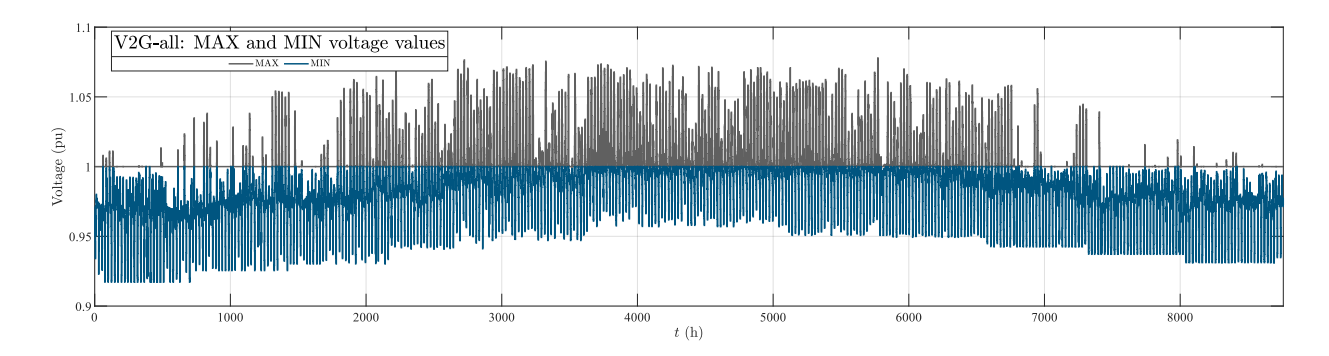


Figure 17: The maximum and minimum values of voltage in Grid 2 over the whole year when EVs (and PVs) are integrated in all homes with the V2G strategy.

8.6 Remarks on EVs and V2G impact on the tested distribution grids

The project developed market algorithms for V1G and V2G charging, considering factors such as home consumption, PV output, driving activity, battery state of charge, and price signals throughout the year. The study concludes that V2G enhances household energy management by reducing peak demand and grid dependence. By storing electricity when prices are low and discharging during high-demand periods, it optimizes costs and improves energy efficiency. It also increases self-consumption of renewable energy, particularly solar PV, by storing excess generation for later use instead of exporting it at lower rates. This results in a more balanced and sustainable household energy profile.

Using the EV activity output from the market algorithm, power flow analyses were conducted on the two tested low-voltage distribution grids. The analyses emphasize the importance of considering voltage stability in EV integration. To address this, the project defines metrics that quantify system voltage stability and robustness over the entire year. The findings show that following market signals can be beneficial for grid stability to various extents. However, in some cases, excessive EV charging or discharging can lead to voltage instability, potentially causing PV-EV disconnections and grid disturbances.

A key factor influencing stability is the amount and type of PV in the system and how well EV activity aligns with PV generation. In Grid 2, PV generation, EV usage, and home consumption were well-balanced, allowing seamless EV integration without voltage issues. However, in Grid 1, voltage problems persisted.

To address these issues, the project introduced an automatic tap changer control at the PCC, which adjusts based on the loading of critical cables. The results demonstrate that this approach effectively mitigates voltage problems, ensuring safe EV integration for both V1G and V2G charging strategies. It should be highlighted that the proposed solution would require investment in control and measurement implementations as well as plenty of careful pre-study to ensure that the appropriate PCC voltage control is applied.

9 PART (A) Frequency Control Assessment with the EV (V2G) Support

9.1 Frequency control in the Nordic Power System

Power system is always exposed to various disturbances. It is essential that it has an ability to appropriately deal with those in such a way that its safe and reliable operation is not endangered. Considering a wide range of dynamic phenomena inherent in a power system, a classification of power



system stability types is introduced (ref. 9, 2021). This section deals primarily with the system's frequency stability and its side-effects on other aspects of system dynamics.

System frequency is a crucial property in AC power systems, reflecting the balance of active power between generation and load (including losses). A common analogy used to illustrate the matter is the balance of a scale, as illustrated in Figure 18. Maintaining frequency within specified limits is essential for both small and large disturbances to ensure the efficient operation of system components.

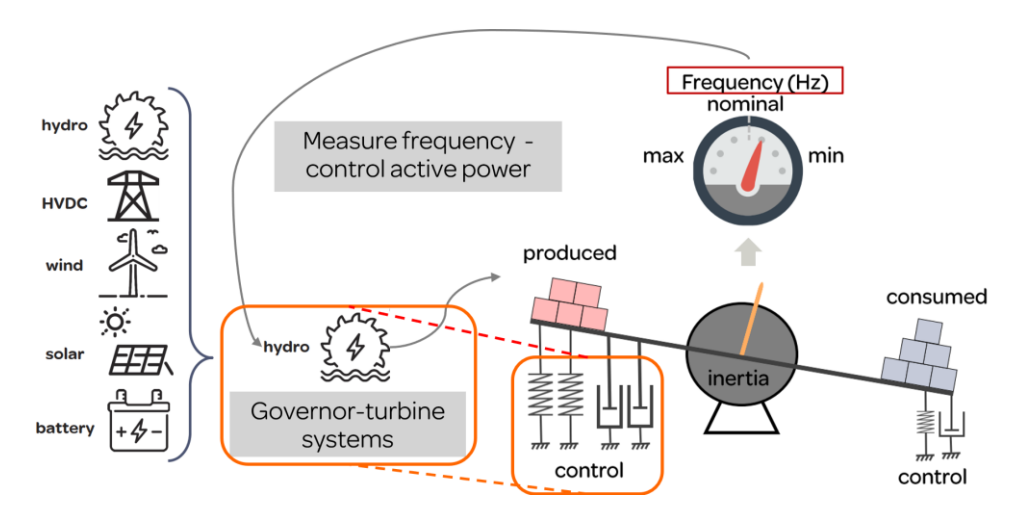


Figure 18: The scale analogy for frequency control and active power balance. In this project, hydro and EV's batteries are utilized.

Frequency controllers are designed to ensure frequency stability objectives and operate based on a specific control strategy. While generator governors (impacting turbine's mechanical power outputs) are commonly used for this purpose, other devices—such as batteries connected via power electronics—can also participate in frequency regulation. Additionally, loads, HVDC links, and renewable energy sources can be similarly utilized for the frequency control service (ref. 10, 2024). These devices could be utilized in various ways, including Frequency Containment Reserves (FCR) and Fast Frequency Reserves (FFR) (ref. 11, 2019). In the NPS, FCR is divided into services for dealing with small (normal) disturbances, named FCR-N, and FCR service for dealing with large disturbances named FCR-D. The details regarding these services can be seen in (ref. 12, 2023).

NPS is a large synchronous electrical grid, consisting of Swedish, Norwegian, Finnish and eastern part of Danish power system. The principles of system operation in the NPS are based on the system operation agreements between the Nordic TSOs: Fingrid, Svenska kraftnät, Statnett, and Energinet (ref. 13, 2023), where the country of responsibility in NPS is illustrated in Figure 19. This system is not synchronized with the rest of Europe, meaning that all power imbalances concern only the frequency behavior within NPS. However, there are multiple HVDC connections with other European countries that enable the exchange of power and energy (ref. 14, 2024).





Figure 19: The map of the NPS with the responsible TSOs. Only the East part of Denmark (the one belonging to the NPS – DK2) is illustrated. The figure is taken from (ref. 15,2023) and adjusted.

Given that EVs have battery storage and are connected to the grid via power electronic inverters, they are also strong candidates for frequency support services. This project focuses on their role in FCR-D analyzing their integration within the NPS test system model in a simulation environment.

Through various control scenarios and a selected test disturbance, the project evaluates the system's need for EV support, as well as the potential benefits and risks associated with their participation in frequency regulation.

9.2 Test system model of Nordic Power System

To investigate the frequency control of NPS in this project, an equivalent model named Nordic 44 (N44) is utilized (ref. 18, 2023). The initial model was developed by STRI in collaboration with the Norwegian University of Science and Technology (NTNU) using the data from Statnett. The N44 model by NTNU is available in PSS®E and DIgSILENT Powerfactory (ref. 17, 2018).

In this project, an equivalent model of the NPS is developed using PSSe software to study the challenges of frequency stability, specifically FCR-D. To highlight emerging frequency stability issues, the system model is configured to operate under the low inertia condition of around 120 GWs (the current estimated minimum) and a relatively high load of approximately 52 GW. The system's kinetic energy is stored in the rotating masses of synchronous generators, as detailed in Table 18 in Annex, which also provides data on power production, maximum power, base power, inertia constants, and FCR-D participation. The installed wind is connected via power electronic converters in 17 units, does not provide any inertia or frequency support, and its data is provided in Table 19 in Annex. The single line diagram of the model is available in (ref. 18, 2023).



For a unit to participate in frequency control, it must meet predefined dynamic performance requirements, which are set by TSOs. In this study, the FCR-D units in the test system feature a HYGOV-type governor-turbine system. The governor parameters are tuned to comply with the latest FCR-D requirements specified in (ref. 12, 2023) and are distributed among 12 synchronous generators, providing a combined regulating strength of approximately 3750 MW/Hz. This exceeds the minimum requirement of 3625 MW/Hz, ensuring that steady-state frequency deviation remains within the allowable limit of 0.5 Hz (from the nominal 50 Hz) following a 1450 MW generator outage—a scenario reflecting the loss of Oskarshamn 3, the largest generating unit disturbance in the NPS. The governor-turbine system parameters are provided in Table 20 in Annex. It should be noted that a slightly higher permanent droop of value 0.1 is chosen to prevent power response saturation after a major disturbance.

Although the FCR-D units meet participation requirements and provide sufficient regulating strength, under low-inertia conditions (such as around 120 GWs) and large disturbances, the system response may still be inadequate, particularly if no additional support is provided to FCR-D.

The operating scenario under investigation assumes a high share of RES in the system. As a result, Oskarshamn 3 is offline, while a significant amount of wind power is active. However, to simulate a dimensioning disturbance, the study considers an outage of both the KVILLDAL 6000 and OULU 7100 generators, representing a total loss of approximately 1450 MW. This disturbance is used to evaluate the system's dynamic behavior and frequency response.

9.3 Test Results: System Frequency Responses after Large Disturbances

This section evaluates the NPS test model dynamics and, more concretely, the frequency responses for different amounts and types of EV frequency support. Initially, the model is tested without EV support to establish the base response. Then, EV frequency control is defined and assessed in relation to its compliance with FCR-D requirements and performance to improve system dynamics. In further steps, the EV FCR-D support is evaluated for different volume contributions and values of control delay.

9.3.1 FCR-D response during low inertia

When no additional EV support is provided, and the system experiences the dimensioning outage of KVILLDAL 6000 and OULU 7100, the frequency deviation from the nominal 50 Hz and the total (summed) FCR-D unit power response are illustrated in Figure 20.

The frequency response highlights two positive aspects:

- The system remains stable.
- The steady-state frequency deviation stays within the allowable limits of ±0.5 Hz.

However, the response also reveals a critical issue: the maximum transient frequency deviation of ±1 Hz is severely exceeded, making the response inadequate. This can be attributed to several factors, including very low inertia, the magnitude of the disturbance, the large water time constant of hydro units (see Table 20), and the absence of additional support from services such as FFR or Emergency Power Control (EPC).

An interesting observation in Figure 20 (right subplot) is the difference between the mechanical and electrical power deviations of the FCR-D units. The mechanical power response exhibits the non-minimum phase property of hydro units, characterized by an initial drop, while the electrical power response shows oscillations following the disturbance. For the system to reach a new steady state, these two power



deviations must ultimately converge, which eventually occurs—matching the disturbance magnitude, adjusted for system losses and load changes.

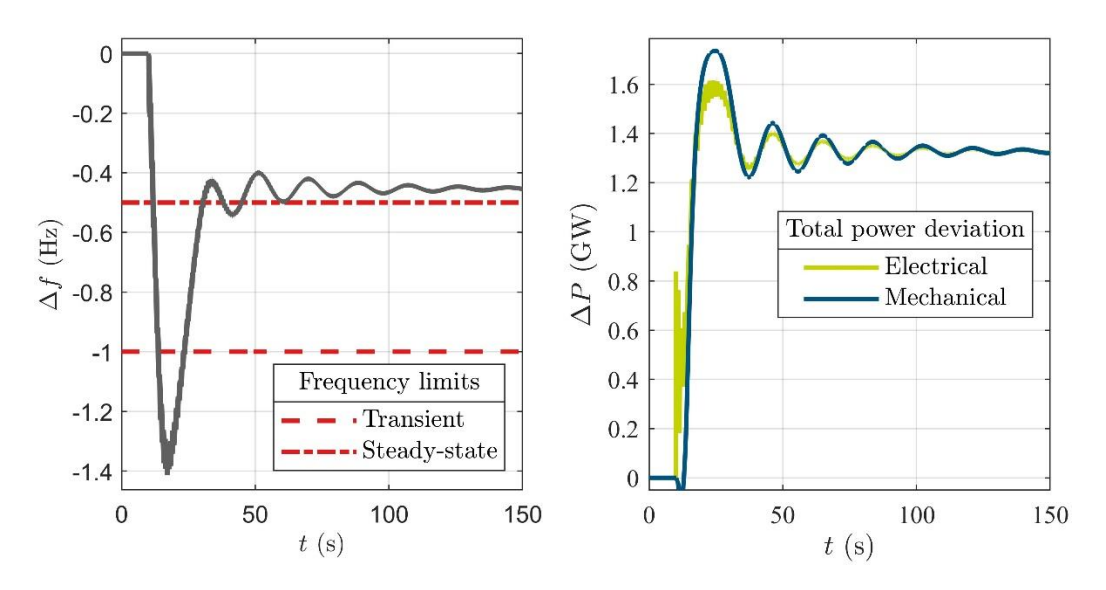


Figure 20: The NPS test model: frequency responses and total FCR-D mechanical and electrical power deviations for the dimensioning disturbance without EV support.

9.3.2 Equivalent Modeling of EVs for Frequency Control

EV charging stations are connected to the low-voltage grid, and their number in the power system is already large and expected to grow further. Modeling each EV individually for transmission system-level studies would be extremely time-consuming. To capture the fundamental and combined effects of EVs in frequency support, this project developed an equivalent battery model representation with a Voltage Source Converter (VSC). The modeling details are provided in (ref. 18, 2023).

This project focuses on EV participation in frequency control, specifically the control loop between frequency measurement and the active power output of the battery. As presented in (ref. 18, 2023), the proposed control design follows a droop frequency-type approach, with the following key properties:

1) Total available power for frequency control:

- The available power cannot exceed the converter power limits.
- It may be lower if there is a risk of excessive energy extraction, leading to a significant reduction in the battery's state of charge.
- It must be high enough to provide adequate power support during large frequency deviations in both directions.
- A fixed or dynamic capacity can be allocated for frequency control, balancing optimal V2G charging/discharging performance. This decision depends on EV owners and their agreements with grid operators.
- o In this project, a constant available EV power value for frequency control is assumed.
- 2) **Time constant of a low-pass filter**: The constant value of 100 ms is assumed for all EVs a typical value assumed for this type of control in high-voltage power electronic applications, and the value needed to filter out the local measurement of the frequency. The value can be different depending on the manufacturers and applications.



- 3) **Dead-band for activation**: In the case of FCR-D EV participation, the dead-band is set for +/- 0.1 Hz
- 4) **Droop constant, or the value that will define regulating strengths in MW/Hz:** Sensitivity studies are used to evaluate this value. Instead of defining an individual droop, the project considers the total regulating strength of all EVs in the system.
- 5) Overall control, communication, and measurement delay:
 - o The reaction time of EVs to frequency deviations remains uncertain.
 - Literature suggests a wide range of possible delays, which will likely depend on the practical implementation of EV frequency control.
 - To address this uncertainty, this project conducts a sensitivity study to assess the impact of delays on frequency control and system stability.

The active power reference for frequency control closely follows the actual power output, considering the battery dynamics defined in (ref. 18, 2023). The equivalent EV models are distributed across seven large battery units within the NPS test system, as detailed in Table 21, with all units participating in FCR-D.

FCR-D step requirement test:

According to (ref. 12, 2023), for a unit to fulfil a dynamic response test, it needs to provide at least 86% of steady-state power (ΔP_{ss}) and 3.2 s $\times \Delta P_{ss}$ of energy output when it is subjected to a frequency ramp input with an amplitude of 0.9 Hz and rate 0.2368 Hz/s.

The equivalent EV battery model built in Simulink (Matlab) is tested in that manner for different amount of control delay in the range from 0 to 2 s in steps of 0.5 s. The model is presented in (ref. 18, 2023). The results in Figure 21 are shown for underfrequency test, from 49.9 Hz to 49.0 Hz where EV battery power is illustrated with different colors.

As expected, higher delays are not favorable since higher values do not provide sufficiently fast responses. Nevertheless, due to a very fast response time of a battery, even with 2 seconds of delay, the full response is provided at the time of 7.5 s after a ramp initiation (690 s in Figure 21).



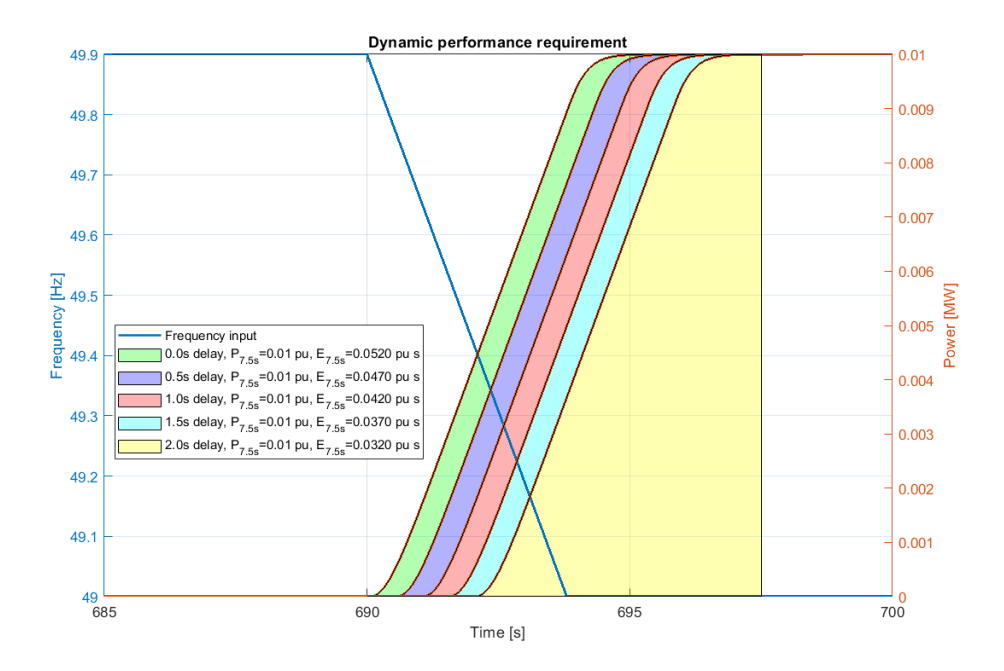


Figure 21: FCR-D ramp test of EV battery dynamic performance for different values of frequency control delays.

The energy output differs among different delay values at the time of 7.5 seconds (697.5 s in Figure 21), but also that part of the requirement is fulfilled for all the tested delays.

Additional remarks:

- The droop constant does not play any role in the ramp performance test because the response increases linearly and has a steady-state contribution; their ratio remains the same.
- Over-frequency tests provide (very much) equivalent results since the battery frequency control is symmetrical and there are no issues with power limitations.

FCR-D stability test:

Another test that a unit needs to fulfill for the FCR-D participation is a closed-loop stability test (ref. 12, 2023). Assuming that the equivalent unit (scaled to a system level) controls the frequency response of a 120 GWs-kinetic energy power system, there should be an appropriate closed-loop stability margin reflecting a circle with a radius of 0.43 and 0.43×0.95 for reduced requirement, in a complex plot with the center in (0,0). Nyquist plot of a closed-loop transfer function shall not cross the defined circle for a system to be defined as robustly stable (ref. 19, 2005). To obtain a Nyquist plot of an EV system model in a real field test, one would need to inject test sinusoidal test signals with various frequencies and record the power outputs. In simulation environments, such as Simulink (Matlab), it is possible to obtain a continuous transfer function of it. In Figure 22, both methods are used for EV models with various delays given for different colors.



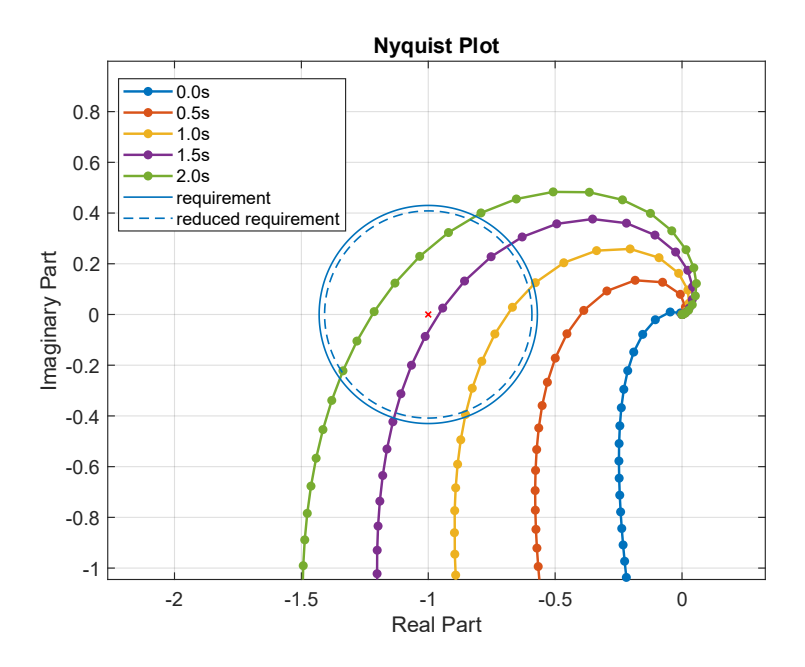


Figure 22: FCR-D stability test of an EV frequency control model with the various frequency control delays.

Figure 22 shows that only delays of 0 and 0.5 seconds meet the stability requirements from the chosen set. Higher delays pose a risk, potentially compromising the system's robust stability.

With a clearer understanding of the acceptable delay range for FCR-D service in EV-based units, the next step is to integrate this support into the developed NPS test model.

9.3.3 EV support to FCR-D during low inertia: system responses

For this analysis, three different delay levels will be examined: 0, 0.5, and 1 second—even though a 1-second delay does not meet the FCR-D stability requirement. The same outage scenario as in the no EV support case will be tested.

The goal is to determine the appropriate level of EV FCR-D support needed to ensure that the transient frequency deviation margin is not exceeded. This can only be achieved by increasing the total EV regulating strength (gain) in MW/Hz and running simulations until the condition is met. The EV frequency control gain is evenly distributed across seven equivalent battery units in the test system.

Figure 23 presents the frequency responses on the left and the total EV frequency support on the right.



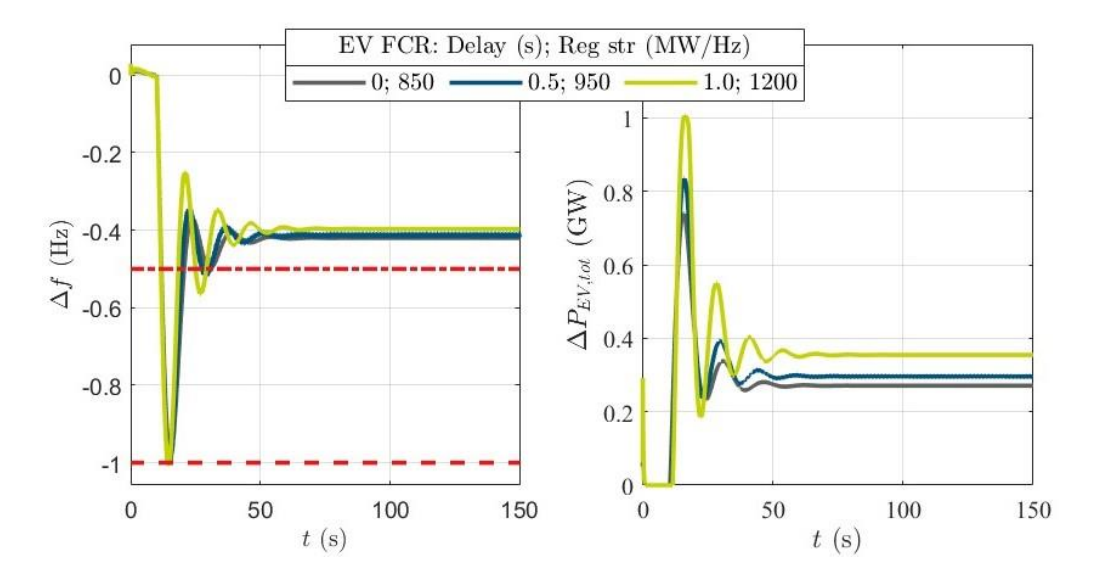


Figure 23: The NPS test model: frequency responses and total EVs power support for the dimensioning disturbance.

The results indicate that EV frequency support, when implemented with appropriately defined gains and all three tested delay values, successfully maintains frequency responses within predefined steady-state and transient margins. However, higher delays lead to increased oscillations and require greater EV frequency control gain (regulating strength in MW/Hz), resulting in a higher power demand in MW.

Note: The system requires initialization at the start of the simulation, but this does not fundamentally impact the results.

The findings in Figure 23 present an optimistic scenario, demonstrating that with an EV FCR-D service delay of 0.5 seconds, a regulating strength of 950 MW/Hz, and 800 MW of support, the system remains frequency stable.

This raises an important question: "How many EVs are needed to provide such a service?"

Assuming EVs in the NPS have an 11-kW connection and can deliver full power when needed, an **estimated 72700 EVs** would be required to provide this service (approximately 800 MW ÷ 11 kW of EVs).

If EV FCR-D delays are reduced, lower regulating strengths and power capacities are needed. In the zero-delay scenario, these values decrease to 850 MW/Hz and 750 MW of power.

Remark: The calculated values assume no other frequency support services are available and that EVs are the sole providers of frequency control. In reality, other support mechanisms—such as HVDC systems, RES, and other battery storage solutions—will contribute. Additionally, hydro governors could be optimized (be more efficient) to reduce the burden on EVs.

Further increasing EV FCR-D support can enhance the frequency response beyond just meeting the minimum requirements. This requires higher regulating strengths. Figure 24 illustrates the frequency responses and EV power support for three increased regulating strengths: 1100, 1300, and 1500 MW/Hz, in the zero-delay scenario.



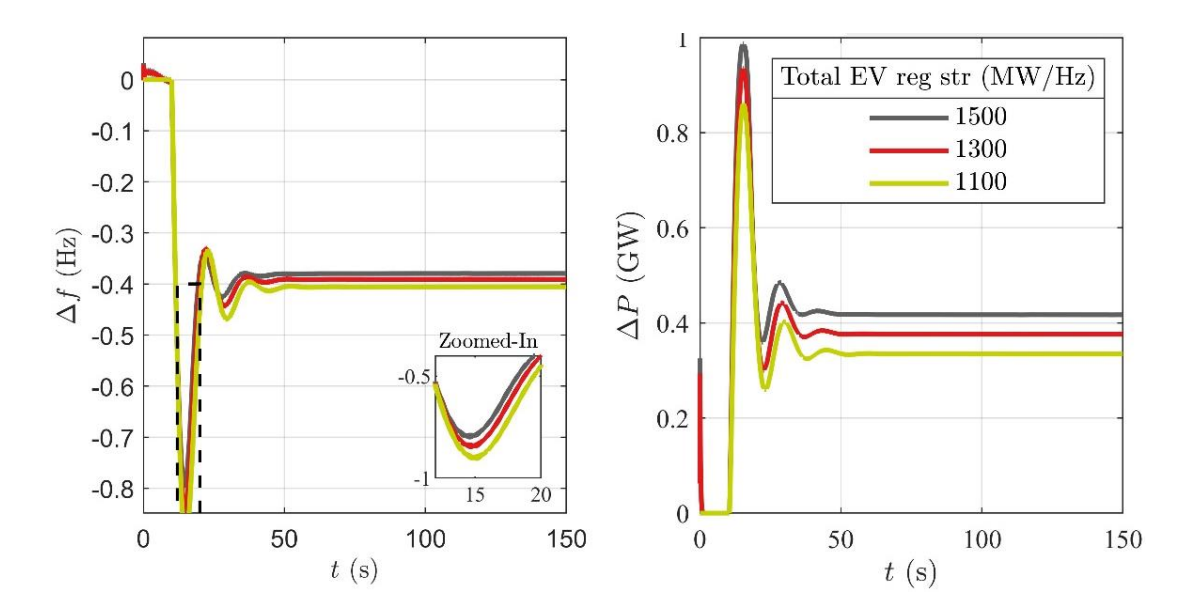


Figure 24: The impact of EVs regulating strengths increase on the system responses when zero EV frequency control delay is present.

Figure 24 confirms that further improvements in frequency response are achievable but come at the cost of higher power contributions from EVs. As a result, TSOs must determine an optimal balance—ensuring robust margin for stable frequency response while minimizing the reserve capacity used, since FCR-D services are compensated through the FCR market.

Figure 25 presents the same analysis with a **0.5-second delay**, leading to an important observation: When a delay is present in EV FCR-D support, even if the requirements are met, it can induce electromechanical oscillations and potentially lead to small-signal instability when higher EV frequency control gains are applied.

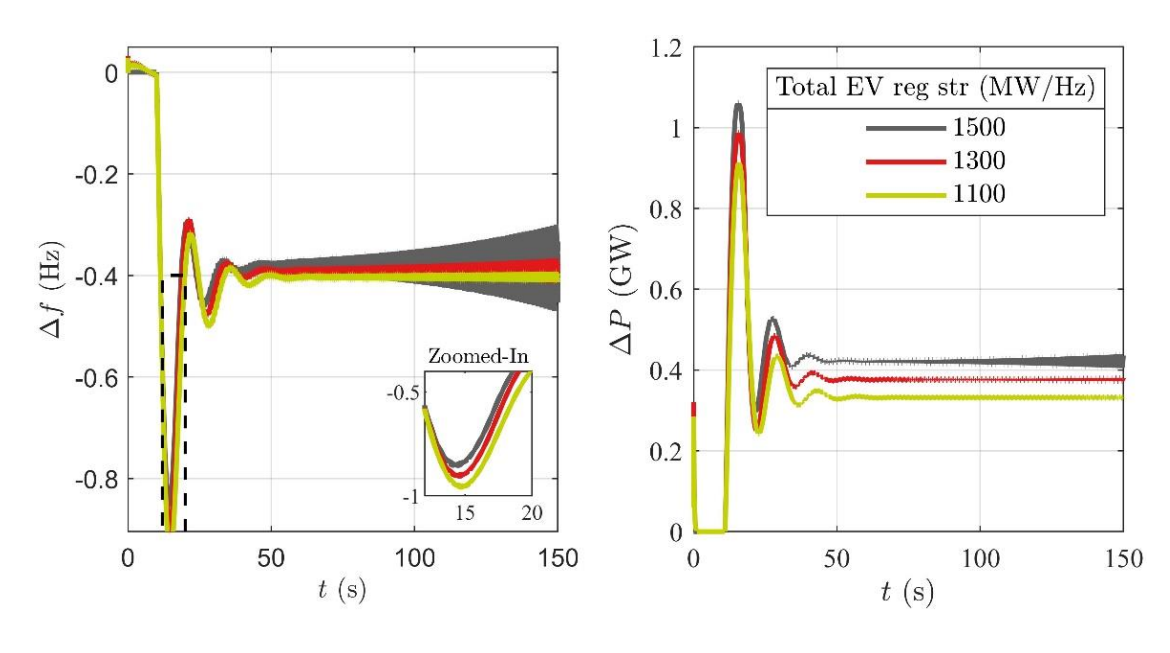


Figure 25: Small-signal instability: the impact of EVs regulating strengths increase on the system responses when 0.5 s EV frequency control delay is present.



This outcome is not unexpected, as in the context of electromechanical oscillations, which occur at higher frequencies, a 0.5-second delay is significant. The associated phase shift can strongly impact damping, particularly for the oscillatory mode affected by the EV FCR-D support.

From the analysis of the obtained frequency signals, it can be seen that the mode of oscillations is around 0.7 Hz, and it represents inter-area oscillations between North/East versus South/West of the NPS. As the EV FCR-D gain is increasing, although the maximum frequency deviation is reducing (see the zoomed-in box in Figure 25), the damping of the inter-area mode is jeopardized from -0.6% to -1.4%, and finally to -2%.

These findings highlight the critical need for an accurate system model when assessing EV frequency support. Simplified models risk overlooking key stability issues and may lead to misleading conclusions.

However, it is important to acknowledge that:

- The observed instability is **based on specific assumptions** used to design the **NPS test model** and **EV frequency support framework**.
- Instability occurs only at high EV control gains, assuming no additional support from other sources.
- A potential mitigation strategy could be the use of a static (feedforward) EV frequency support method, though this would require further validation and definitely a compensation for the "lost" feedback.

Ultimately, these results serve as a valuable insight for those considering EV-based frequency support. They emphasize the importance of minimizing control, communication, and measurement delays to reduce the risk of unintended instability.

9.4 Remarks on EVs frequency support during low inertia in the NPS test model

The analysis demonstrated that EVs can be successfully integrated into the NPS test model for FCR-D service. The model was carefully designed to replicate a challenging scenario and disturbance event in the NPS, allowing the effects of EV support to be highlighted and various key aspects to be studied. The assumed EV frequency control was based on frequency feedback and a droop-type design.

The results showed that, due to their power electronic converters, EVs provide significantly faster frequency response than hydro generators, leading to noticeable improvements in system stability. This includes reducing transient frequency deviations and damping oscillations as the system moves toward a new steady state. The study quantified the MW and MW/Hz required for such a service under challenging conditions, as well as the equivalent number of EVs needed to provide this support, which could be around 70,000 units. However, it is important to note that this support is not strictly required—TSOs ultimately decide how much EV (or battery-based) support should be utilized and how much should come from other reserves, such as HVDC, wind power, or demand-side response.

One particularly interesting aspect of the analysis was the impact of delays in EV frequency control. The results showed that while certain delay values, such as 0.5 seconds, do not necessarily disqualify a unit from meeting FCR-D participation requirements, they could introduce potential stability risks. The development of large-scale test models, such as the one in this project, ensured that electromechanical oscillations were captured, allowing their interaction with EV frequency control to be studied in detail.



The findings indicate that when EVs contribute significantly to frequency control, the presence of a control delay can lead to small-signal instability. This is a crucial insight that could motivate TSOs to carefully assess control system delays to prevent any unintended negative effects on grid stability.

10 PART (B): Replication of Energy Planning Tool (T2.6) in Gothenburg Pilot

10.1 Introduction

10.1.1 Context, objectives and relation to other tasks and WPs

This section aims to present insights from the replication of the Energy Planning Tool, developed and reported by CERTH in T2.6, to efficiently address the specific objective described in the Grant Agreement for SCALE WP5: to exploit a planning tool which integrates EV mobility and charging infrastructure rollout in combination with grid congestion.

In T2.6, CERTH combined:

- i) EV user mobility patterns from a developed transport model,
- ii) charging infrastructure rollout optimisation algorithms, and
- iii) component-based dynamic grid modelling,

into an integrated approach for evaluating smart charging and V2G strategies in the cities participating in SCALE as demonstration sites.

Beyond supporting the WP5 objective, the development of the tool also contributes to the broader SCALE objective: to optimally leverage existing grid infrastructure, focusing on limiting grid congestion and enabling citizens to act as prosumers. During T2.6, the tool was initially applied to a LV DN in Utrecht. A key challenge, as stated by the Grant Agreement, is to assess the tool's replicability, scalability and adoptability on a larger scale. T5.2 addresses this challenge by presenting the application and results of the tool in the model of a medium-voltage (MV) DN of the Chalmers University of Technology campus, within the SCALE Gothenburg pilot.

10.1.2 Overview of applied methodology

A brief overview of the tool methodology, reported in detail in D2.6 (20, 2025), and the required modifications for its application in the respective DN model of Chalmers University of Technology in Gothenburg campus is presented in this paragraph. To comprehensively evaluate the performance of smart charging and V2G solutions, CERTH developed multiple charging scenarios representing diverse real-world conditions. Each scenario reflects different user behaviours, station types, and temporal demand patterns—ranging from predictable home charging routines to irregular highway or public charging events. This variety is essential to test the adaptability and resilience of our solutions under varying loads, geographic contexts, and usage intensities to support mass scalability of EVs. By incorporating multiple scenarios, we ensure that the model can capture edge cases, stress-test system responses, and provide insights that are both robust and broadly applicable to future mobility and energy systems. Thus, the adopted scenario-based analysis contributes valuable insights to support the large-scale deployment of V2G charging infrastructure.



The transport model in this context simulates the movement and charging behaviour of electric vehicles across time and locations for different charging strategies (charging at night or at work, opportunistic charging, etc.). It is grounded in well-established probabilistic methods, particularly the normal distribution, which reflects real-world variability in arrival and departure times, thus creating the opportunity time windows for charging. This approach ensures the model is both realistic and statistically valid, closely mirroring actual user behaviour at different types of charging stations—residential, public, and highway. By capturing these temporal and spatial patterns accurately, the model enables robust testing of smart charging and Vehicle-to-Grid (V2G) solutions. Its benefits include improved grid load forecasting, energy management, and infrastructure planning, making it a critical tool for evaluating the scalability and effectiveness of advanced EV charging strategies under diverse, lifelike conditions.

Based on mobility patterns, CERTH developed the core algorithms of the Energy Planning Tool that calculate the optimal location, rated power, and operating strategy of charging stations within an electrical DN – in this particular case, at Chalmers University of Technology campus in Gothenburg. The implementation of the optimisation algorithm was based on solving the power flow equations within the network, with the objective of reducing overall congestion and total network losses, without violating line loading limits or node voltage limits. Having on the one hand the power flow equations that are non-linear and on the other the hybrid form of the solution space to be investigated, i.e. number of EV chargers and bus number to be connected, integers, and the rated power, real number, the problem is described as Mixed-Integer Non-Linear (MINLP), that are classified as NP hard. For its solving, meta-heuristic algorithms have been employed by CERTH utilizing the **pymoo** (21, 2020) and the **pandapower** libraries (22, 2018) in Python, which are well-suited for solving such optimization problems with high precision. As a result, the solutions provided regarding the location, rated power, and operation of the charging stations are quite accurate and significantly better than those obtained through linear approximations. Additionally, for numerical execution reasons, the State of Charge (SoC) is considered to be zero when no vehicle is connected to a charger, meaning that the charger is not operating under those conditions.

Finally, the exported mobility patterns, optimised charging infrastructure locations, and V2G optimal power exchange scheduling are imported into the dynamic model of the grid. To stress-test system dynamic response in a holistic approach, non-idealised, high-fidelity models have been used for the representation of all system components, i.e., the electrical grid, the V2G charger (including its controller and power electronics) and the EV powertrain battery. On top of that, for all components, misleading oversimplifications have been avoided and model dependencies to varying system variables have been considered to ensure the capturing of nonlinear dynamic phenomena. For all component models a Modelica model library created by CERTH has been used. System specifications, such as line characteristics, load demand timeseries and slack operation have been provided by Chalmers.

An overview of the applied methodology is presented in Figure 26.



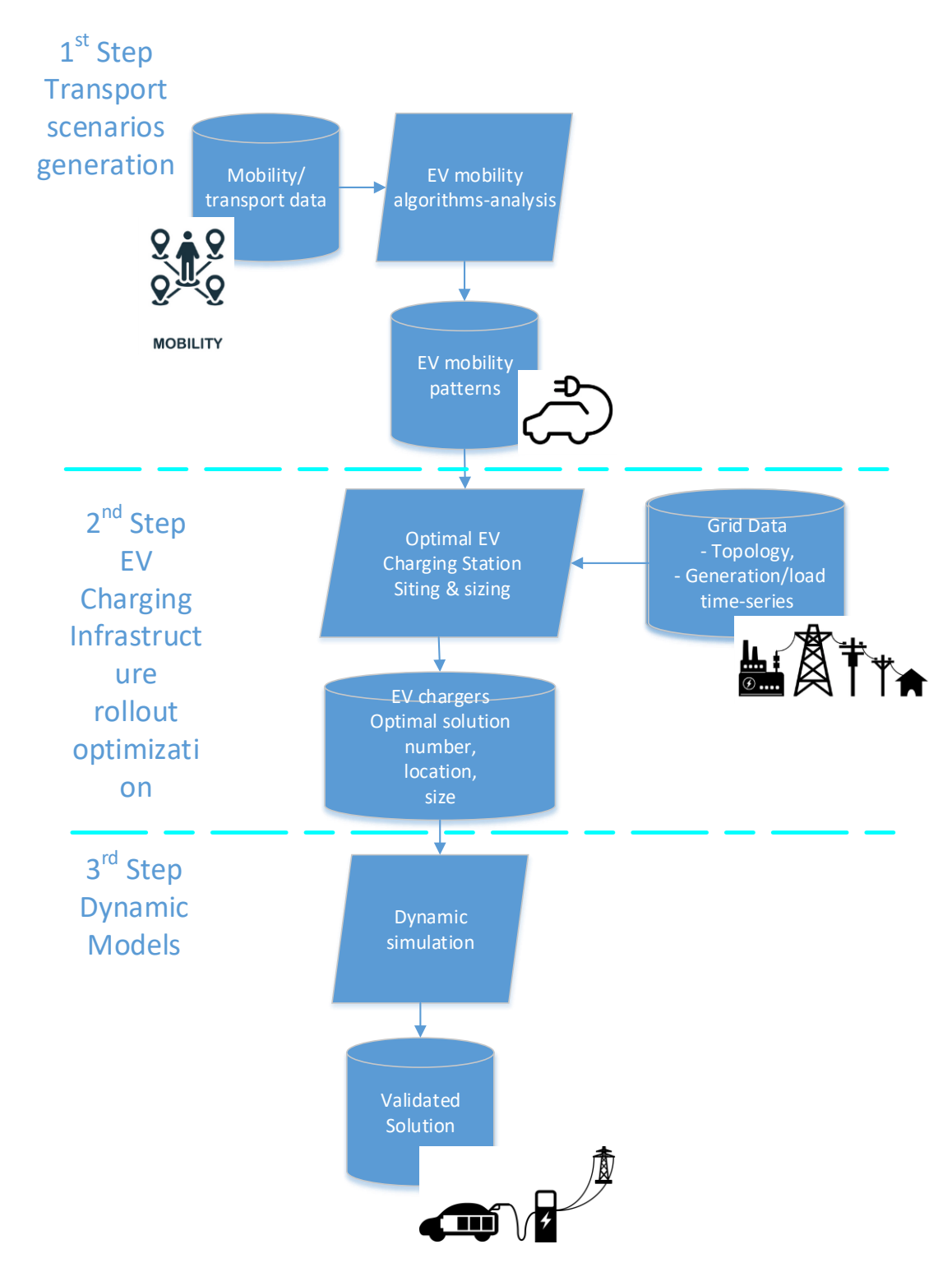


Figure 26: Overall methodology of CERTH's Energy Planning Tool

10.1.3 System description

The Chalmers University of Technology in Gothenburg is a MV DN, operating at a nominal voltage of 10.5 kV and a frequency of 50 Hz. It comprises of:



- 23 MV buses,
- 22 power lines connecting the buses,
- 30 LV loads with a nominal voltage of 400 V,
- 40 distribution transformers connecting the LV loads to the MV network. The nominal voltage rating of the transformers is 10.5/0.4 kV.

The existing topology of the system under study is illustrated in Figure 27. System nodes are depicted as green circular signs. Each node is labelled with its corresponding name, as provided by the Pilot. It should be noted that nodes 07:8.1, 07:8.1.1, 07:8.1.2, 07:8.1.3, 07:8.1.1.1, which are connected to 07:8 (serving as the slack bus), are not visible on the map due to having identical geolocation data with node 07:8.

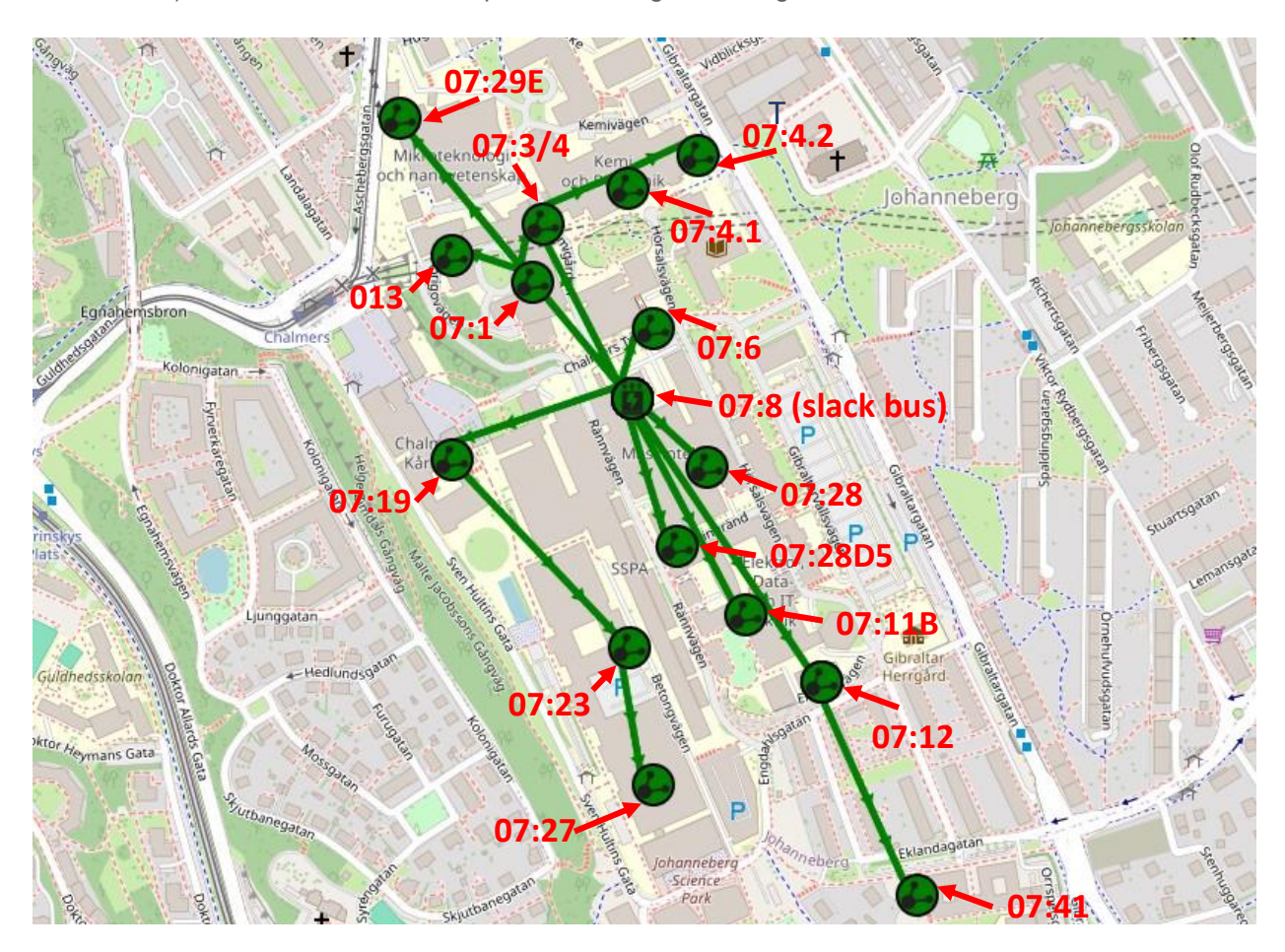


Figure 27: Schematic representation of the current topology of the grid under study

10.2 Definition of transport scenarios

In modelling EV charging behaviour, it is crucial to accurately capture the temporal patterns of when and where vehicles are being charged. Charging stations vary widely in their usage, from residential homes to public locations like shopping malls and highways, each presenting a unique set of behaviours for when EVs arrive and depart.

In order to feed EV charging scenarios into the Energy planning tool, developed by CERTH, as shown in Figure 26, our approach of modelling them was designed to reflect realistic usage patterns, grounded in



empirical data drawn from the Utrecht Use Case. These charging profiles are essential for scenario planning, particularly when projecting transformer load capacity and evaluating the impact of different EVCI topologies.

To model these charging scenarios effectively, we rely on probabilistic methods, particularly **normal distribution**, as the primary tool for generating realistic arrival and departure times. The normal distribution is widely used in statistical modelling due to its ability to represent real-world phenomena where events cluster around a central value with natural variation on either side. It forms a bell curve, where most data points (in this case, arrival or departure times) are centred around the average, but there are still occurrences of early or late events. This shape matches many of the charging behaviours observed in real life.

The scenarios are presented in the following paragraphs.

10.2.1 Scenario 1: workplace charging

Workplace charging, presented in Figure 28, is typically used by individuals who drive to work and stay for a full workday. The arrival times reflect the common start times for office work, typically between 7:00 AM and 9:00 AM. Departure times are set between 4:00 PM and 6:00 PM, aligning with typical end-of-day work hours. The duration of charging, from 8 to 11 hours, reflects the length of an average workday, including some flexibility for late arrivals or early departures.

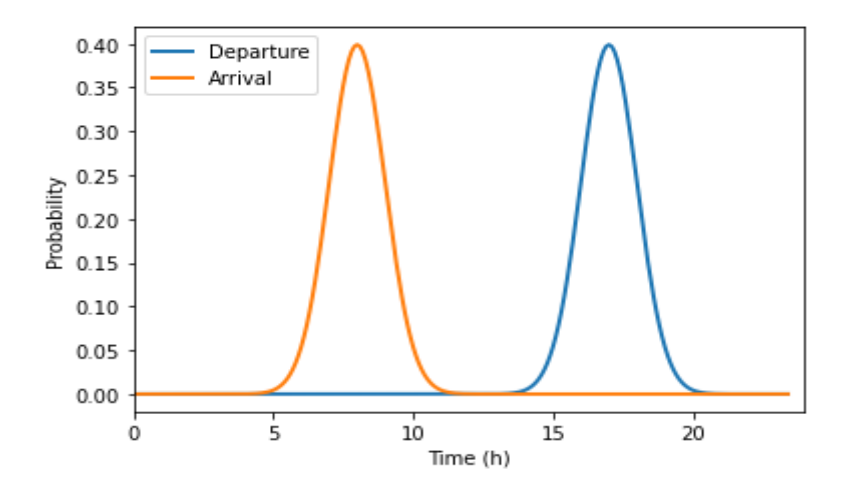


Figure 28: Workplace charging scenario

10.2.2 Scenario 2: residential charging

Residential charging, presented in Figure 29, happens primarily overnight when most people return home from work. Arrival times are modelled between 6:00 PM and 9:00 PM, reflecting the typical hours people return home. Departure times are set for the early morning, between 6:00 AM and 8:00 AM, which corresponds to when most people leave for work.



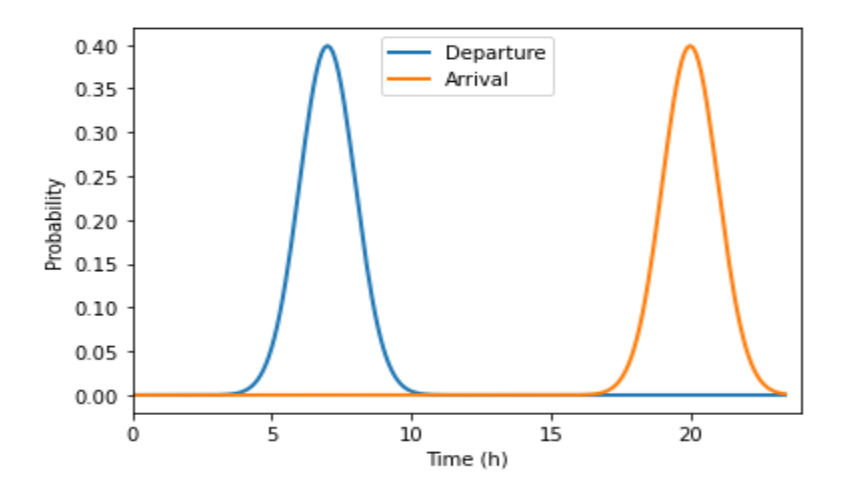


Figure 29: Residential charging scenario

10.2.3 Scenario 3: public charging (shopping malls, restaurants)

Public charging stations at shopping malls and restaurants typically experience activity around lunchtime and evening hours. These two windows, 11:00 AM to 2:00 PM and 5:00 PM to 8:00 PM, align with peak shopping and dining periods. Distributions are plotted in Figure 30.

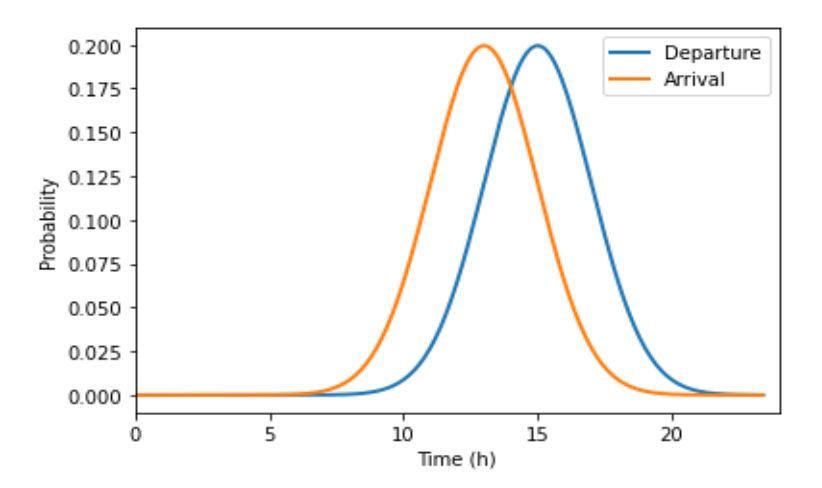


Figure 30: Public charging scenario

10.2.4 Scenario 4: fast charging stations (highways, busy urban areas)

Fast charging stations are designed for short, quick charging sessions, primarily used during commuting hours or on long trips. Peak arrival times are set for rush hours in the morning (7:00 AM to 9:00 AM) and evening (5:00 PM to 7:00 PM), when drivers are most likely to stop briefly (30 minutes to 1 hour) to recharge their vehicles. This is evident in Figure 31.



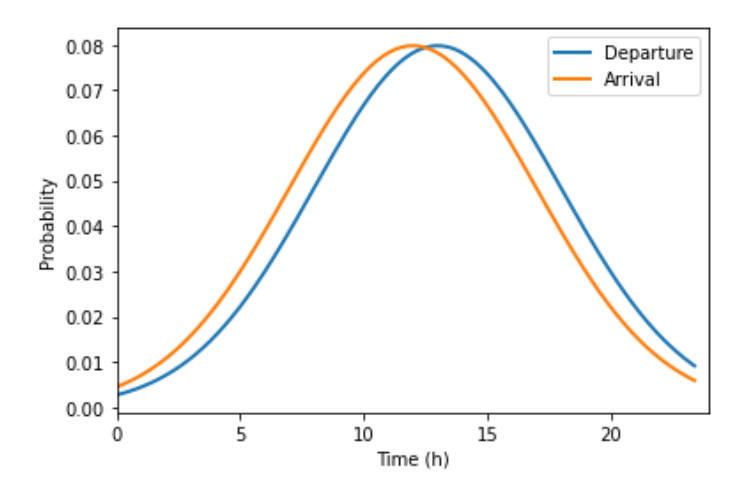


Figure 31: Fast charging scenario

10.2.5 Scenario 5: event charging (concerts, sports events)

Charging at event locations like concerts or sports arenas typically sees concentrated arrival and departure times. Events usually start around 6:00 PM or 8:00 PM, with attendees arriving beforehand. Departure is modelled between 10:00 PM and 12:00 AM, after the event ends (see Figure 32).

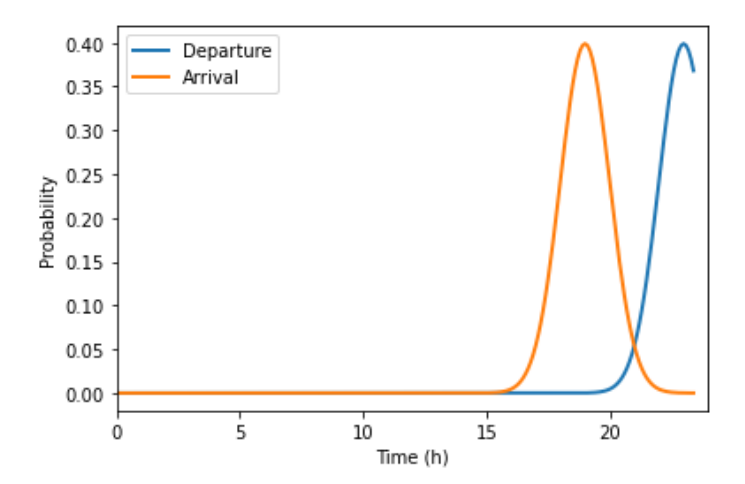


Figure 32: Event charging scenario

10.2.6 Scenario 6: fleet charging (taxi services, delivery vehicles)

Fleet vehicles, such as taxis and delivery vans, often recharge during the night when they are out of service. The modelled arrival time is set between 2:00 AM and 4:00 AM, and departure occurs just before service begins in the early morning (between 6:00 AM and 8:00 AM), as plotted in Figure 33.



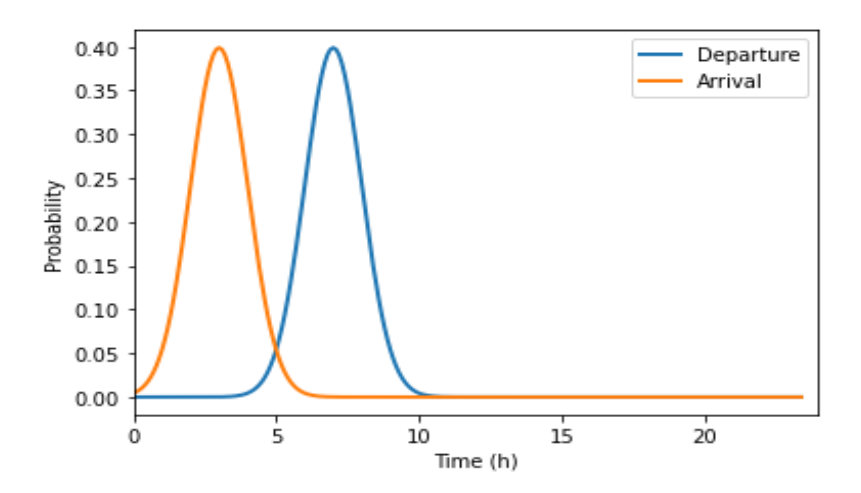


Figure 33: Fleet charging scenario

10.2.7 Scenario 7: hotel charging

Hotel guests typically park their cars overnight. Arrival times are modelled between 8:00 PM and 11:00 PM, reflecting when guests check-in, and departure occurs the next morning between 7:00 AM and 9:00 AM. This pattern is presented in Figure 34.

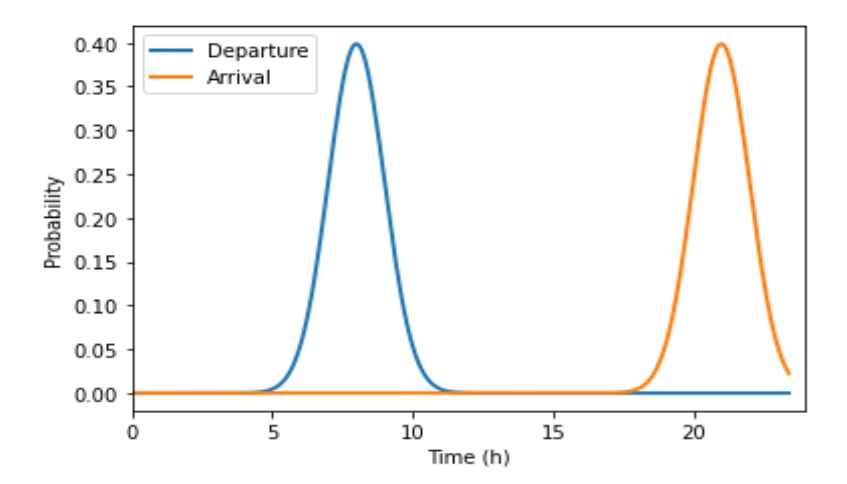


Figure 34: Hotel charging scenario

10.2.8 Scenario 8: university campus charging

University students and staff typically arrive at campus in the morning, between 8:00 AM and 10:00 AM, and leave in the late afternoon or early evening, between 4:00 PM and 6:00 PM, as presented in Figure 35.

WWW.SCALE.EU _______ 50



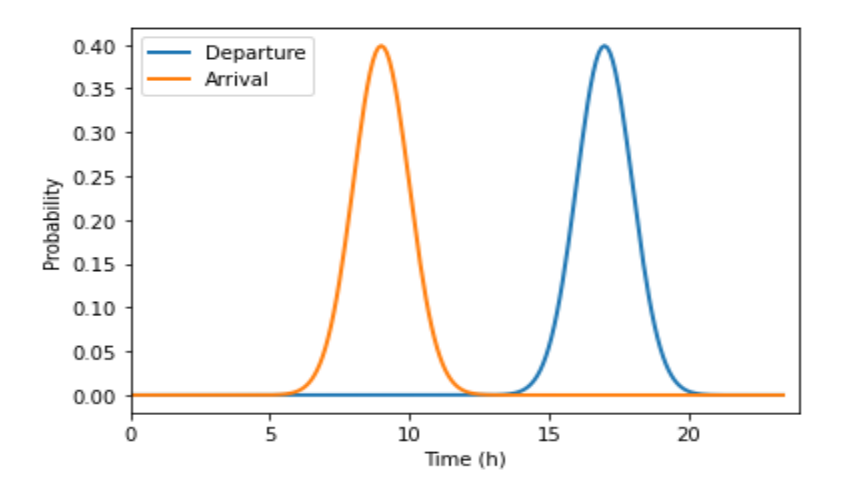


Figure 35: University campus charging scenario

10.2.9 Scenario 9: weekend outing charging (parks, tourist attractions)

Weekend outings, such as trips to parks or tourist spots, tend to have a mid-morning arrival time (10:00 AM to 12:00 PM) and an afternoon departure time (4:00 PM to 6:00 PM). A longer duration of 4 to 8 hours reflects the typical time spent at these locations. This pattern is shown in Figure 36.

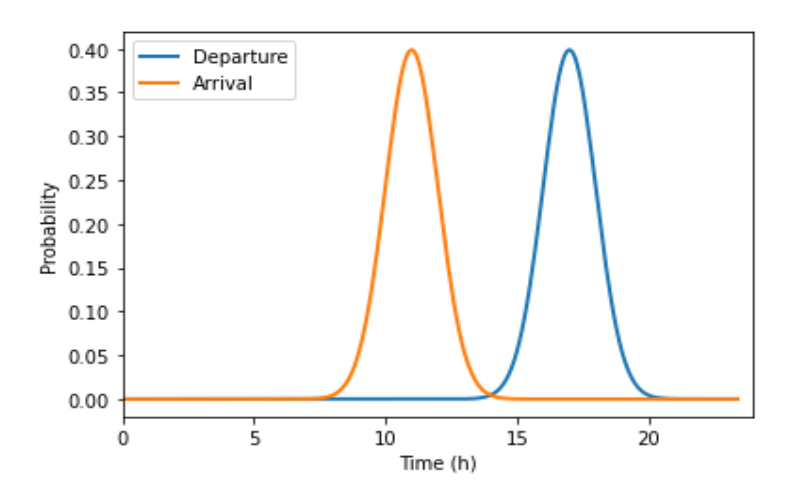


Figure 36: Weekend outing charging scenario

All charging scenarios are summarized in Table 7.



Table 7: Summary List of charging scenarios based on mobility pattern

Charging Scenario	Arrival time	Departure time	Duration
1. Workplace	Between 7:00 AM and 9:00 AM	Between 4:00 PM and 6:00 PM	8 to 11 hours
2. Residential	Between 6:00 PM and 9:00 PM	Between 6:00 AM and 8:00 AM	9 to 12 hours
Public (shopping malls, restaurants)	Between 11:00 AM and 2:00 PM or 5:00 PM and 8:00 PM	1 to 3 hours after arrival	1 to 3 hours
4. Fast (highways, busy urban areas)	Between 7:00 AM and 9:00 AM or 5:00 PM to 7:00 PM	30 minutes to 1 hour after arrival	30 minutes to 1 hour
5. Events (concerts, sports)	Between 6:00 PM and 8:00 PM	Between 10:00 PM and 12:00 AM	3 to 5 hours
6. Fleet (taxi, delivery services)	Between 2:00 AM and 4:00 AM	Between 6:00 AM and 8:00 AM	2 to 6 hours
7. Hotel	Between 8:00 PM and 11:00 PM	Between 7:00 AM and 9:00 AM	8 to 12 hours
8. University Campus	Between 8:00 AM and 10:00 AM	Between 4:00 PM and 6:00 PM	6 to 10 hours
Weekend outing (parks, tourist attractions)	Between 10:00 AM and 12:00 PM	Between 4:00 PM and 6:00 PM	4 to 8 hours



10.3 EV charging infrastructure (EVCI) rollout optimisation

CERTH has utilized the Energy Planning Tool, as documented in D2.6, to optimize the rollout of electric vehicle charging infrastructure (EVCI). This tool has been tested on MV DN of the Chalmers University of Technology in Gothenburg.

For each of the nine transportation scenarios, the Energy Planning Tool determines the optimal number, nominal power, location, and daily schedule of EV charging stations within the DN. The optimal schedule is calculated in 15-minute intervals throughout the day. The outcome can be provided for any period of the following: daily, weekly, monthly, or annually, depending on the available data of the area and the DN.

The tool optimises these parameters by minimising total daily grid congestion and line power losses while ensuring the grid operates within normal conditions. The tool focuses on the smooth operation of the grid, while taking into consideration EV charging limitations or end-user requirements, such as time of arrival and departure, SoC at the time of arrival and required SoC at the time of departure, as demanded by the end-user, i.e., the EV owner or driver (23, 2024).

In spite of the transportation scenarios being stochastic in nature, the optimized solution reached in each of them, needs to meet the objective and satisfy the constraints set by both the DSO and the EV owner. Thus, the end result reached is the one that meets those criteria.

The following sections present a chart with the SoC of vehicles connected to each installed charging station and a table with the position and the nominal power of the charging stations, for each of the transport scenarios, as presented in the previous section.

10.3.1 Scenario 1: workplace charging

Table 8: Position and nominal power of the chargers for workplace charging scenario

Charging Station	Bus Name	Nominal Power (kVA)
cs13	07:28D5	22
cs14	07:8	22
cs19	07:8.1.1.1	22





Figure 37: Grid Topology with installed charging stations for workplace charging scenario

For this particular scenario, three EV chargers are proposed connected in three nodes of the local DN, having the same nominal power.

10.3.2 Scenario 2: residential charging

Table 9: Position and nominal power of the chargers for residential charging scenario

Charging Station	Bus Name	Nominal Power (kVA)
cs8	07:8.1.1	22
cs15	07:11B	22
cs20	07:28	22



Figure 38: Grid topology with installed charging stations in residential charging scenario

In this scenario, just two EV chargers are recommended to be installed, again as it so happens with the same nominal power and connected on two different nodes, as evidenced in the table and figure above.



10.3.3 Scenario 3: public charging (shopping malls, restaurants)

Table 10: Position and nominal power of the chargers for public charging scenario

Charging Station	Bus Name	Nominal Power (kVA)
cs0	07:28	22
cs9	07:8	22
cs17	07:8.1.1	22



Figure 39: Grid topology with installed charging stations for public charging scenario

In this scenario, again three EV chargers are recommended to be installed, again as it so happens with the same nominal power and connected on different nodes, as evidenced in the table and figure above.

10.3.4 Scenario 4: fast charging stations (highways, busy urban areas)

Table 11: Position and nominal power of the chargers for fast charging scenario

Charging Station	Bus Name	Nominal Power (kVA)
cs11	07:35	22
cs13	013	22





Figure 40: Grid topology with installed charging stations for fast charging scenario

In this scenario, two EV chargers are recommended to be installed, again as it so happens with the same nominal power and connected on different nodes, as evidenced in the table and figure above.

10.3.5 Scenario 5: event charging (concerts, sports event)

Table 12: Position and nominal power of the chargers for event charging scenario

Charging Station	Bus Name	Nominal Power (kVA)
cs2	07:8.1.1.1	22
cs22	07:28D5	22

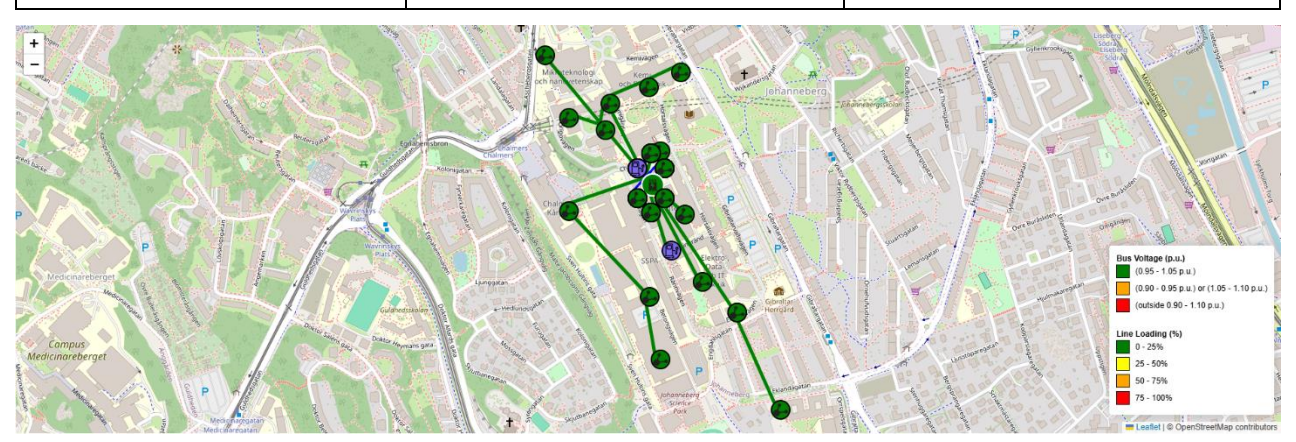


Figure 41: Grid Topology with installed charging stations for event charging scenario

In this scenario, again two EV chargers are recommended to be installed, again as it so happens with the same nominal power and connected on different nodes, as evidenced in the table and figure above.

10.3.6 Scenario 6: fleet charging (taxi services, delivery vehicles)

Table 13: Position and nominal power of the chargers for fleet charging scenario

Charging Station	Bus Name	Nominal Power (kVA)



cs5	07:8	22
cs7	07:8.1	22
cs11	07:8.1.1	22
cs13	07:8.1.2	22
cs14	07:8.1.3	11



Figure 42: Grid topology with installed charging stations for Fleet charging scenario

In this scenario, a total of five EV chargers are recommended to be installed connected on different nodes, as evidenced in the table and figure above.

10.3.7 Scenario 7: hotel charging

Table 14: Position and nominal power of the chargers for hotel charging scenario

Charging Station	Bus Name	Nominal Power (kVA)
cs6	07:6	11
cs21	07:6	22





Figure 43: Grid topology with charging stations for hotel charging scenario

In this scenario, again two EV chargers are recommended to be installed, with nominal power 11 and 22 kVA and connected on same node, as evidenced in the table and figure above.

10.3.8 Scenario 8: university campus charging

Table 15: Position and nominal power of the chargers for university campus charging scenario

Charging Station	Bus Name	Nominal Power (kVA)
cs7	07:4.2	22
cs19	07:8.1.1	22



Figure 44: Grid Topology with installed charging stations for university charging scenario

In this scenario, again two EV chargers are recommended to be installed, again as it so happens with the same nominal power and connected on different nodes, as evidenced in the table and figure above.

10.3.9 Scenario 9: weekend outing (parks, tourists' attractions)

Table 16: Position and nominal power of the chargers for weekend outing charging scenario

Charging Station	Bus Name	Nominal Power (kVA)
cs11	07:8.1.1	22



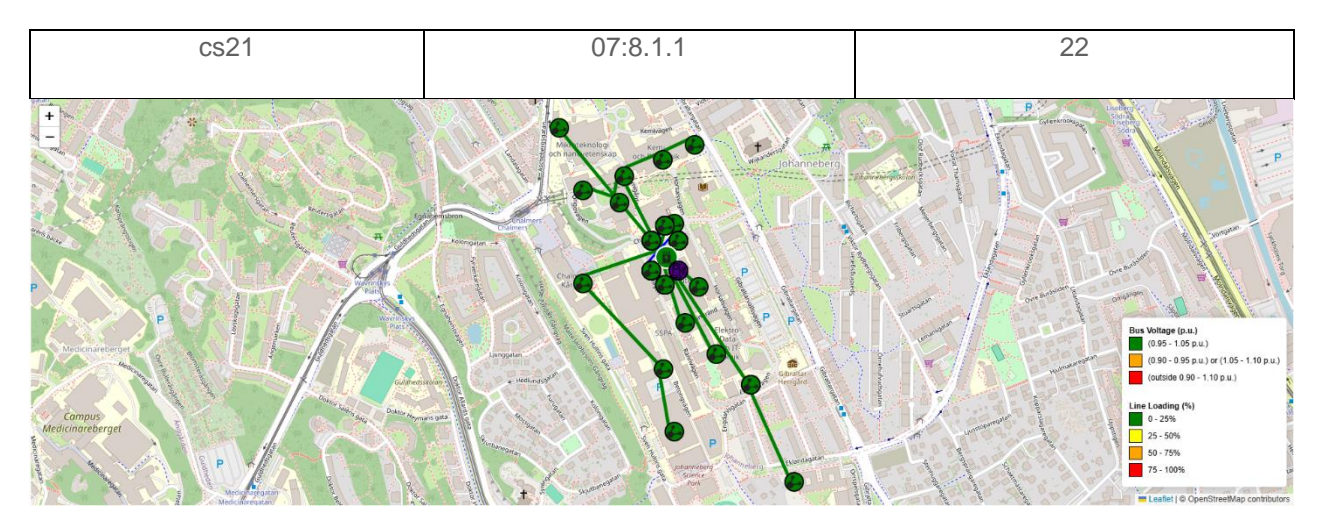


Figure 45: Grid Topology with charging stations for weekend outing charging scenario

In this scenario, the Energy Planning Tool introduces two charging stations on the bus named 07:8.1.1. Each charging station has a nominal power of 22 kVA.

Figure 46 presents the SoC as seen from the EV chargers' point of view, for all scenarios. Assuming that for any SoC value to be detected an EV needs to be connected and charging to a particular EV charger, prior and after the charging session of the EV, the SoC, for the point of view of the EV charger, goes to zero, awaiting the next session.

Any fluctuations detected in the SoC is due to the consideration of V2G mode, for the optimized results. Thus, when connected to the charger, the EV battery can either charge or discharge.



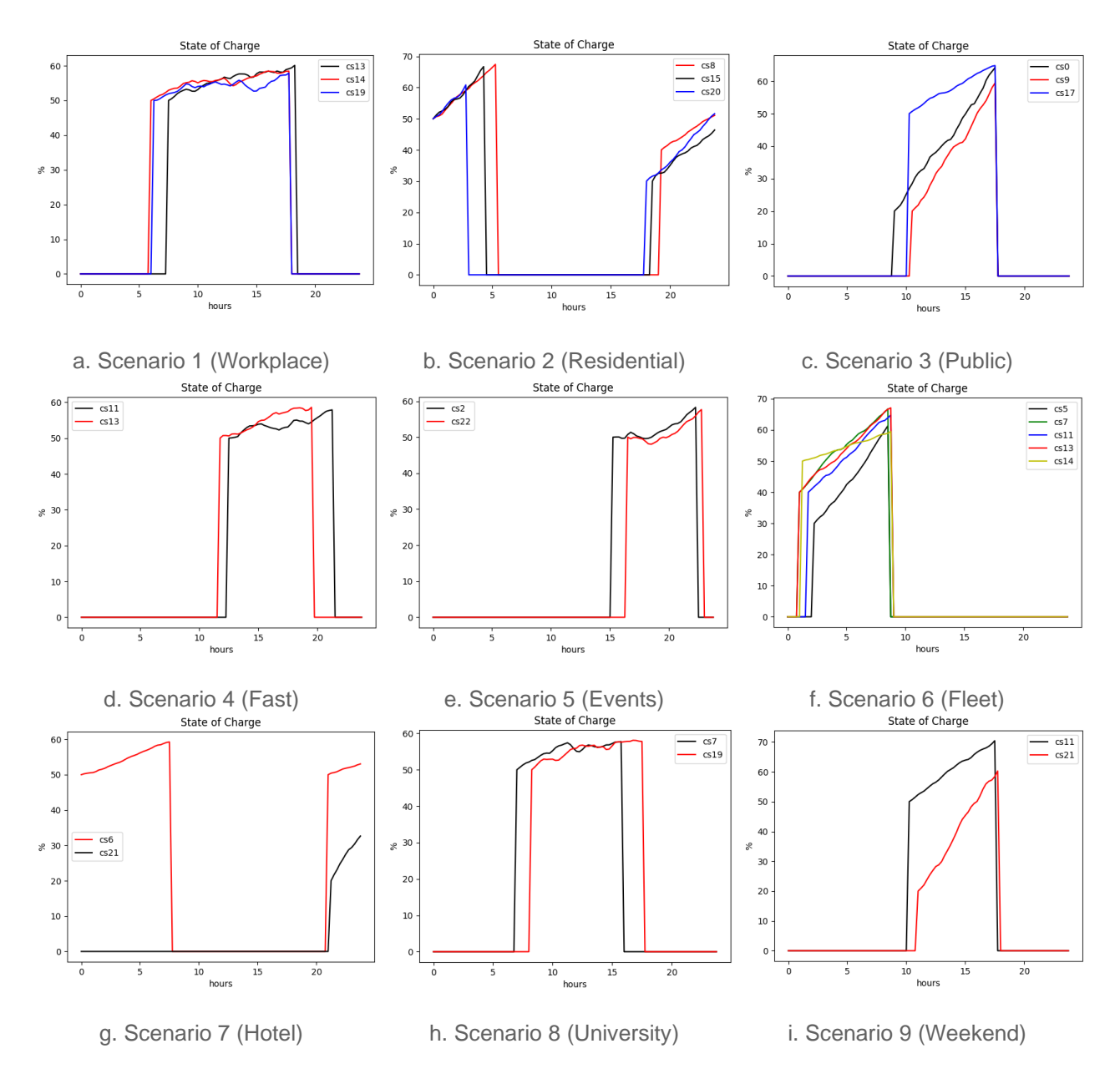


Figure 46: State of charge for all scenarios from the chargers' point of view

10.3.10 Results

The aggregate results for each scenario are summarised in Table 17. Judging by the results, the most desirable connection to the grid are the nodes near to the central substation of the campus site with a common size of 22 kVA. This is due to the required charging demand by the EVs and the requirement of the Energy planning tool to avoid congestion and reduce the losses to the grid. By connecting close to the central substation all those requirements are met, thus the evidences outcome.



Table 17: Summary of optimal charging infrastructure location results

Charging scenario	Optimal location of chargers	Nominal power of chargers (kW)
	07:28D5	22
1. Workplace	7:08	22
	07:8.1.1.1	22
2. Decidential	7:08	11
2. Residential	07:08.1.1	11
	7:28	22
3. Public	7:08	22
	07:08.1.1	22
4 Foot	7:35	22
4. Fast	0.13	22
5. Event	07:08.1.1.1	22
	07:28D5	22
6. Fleet	7:08	22
	07:08.1	22
	07:08.1.1	22
	07:08.1.2	22
	07:08.1.3	11
7 Hotel	7:08	11
7. Hotel	07:08.1	11
O University semant	07:04.2	22
8. University campus	07:08.1.1	22
0 Wookand auting	07:08.1.1	22
9. Weekend outing	07:08.1.1	22



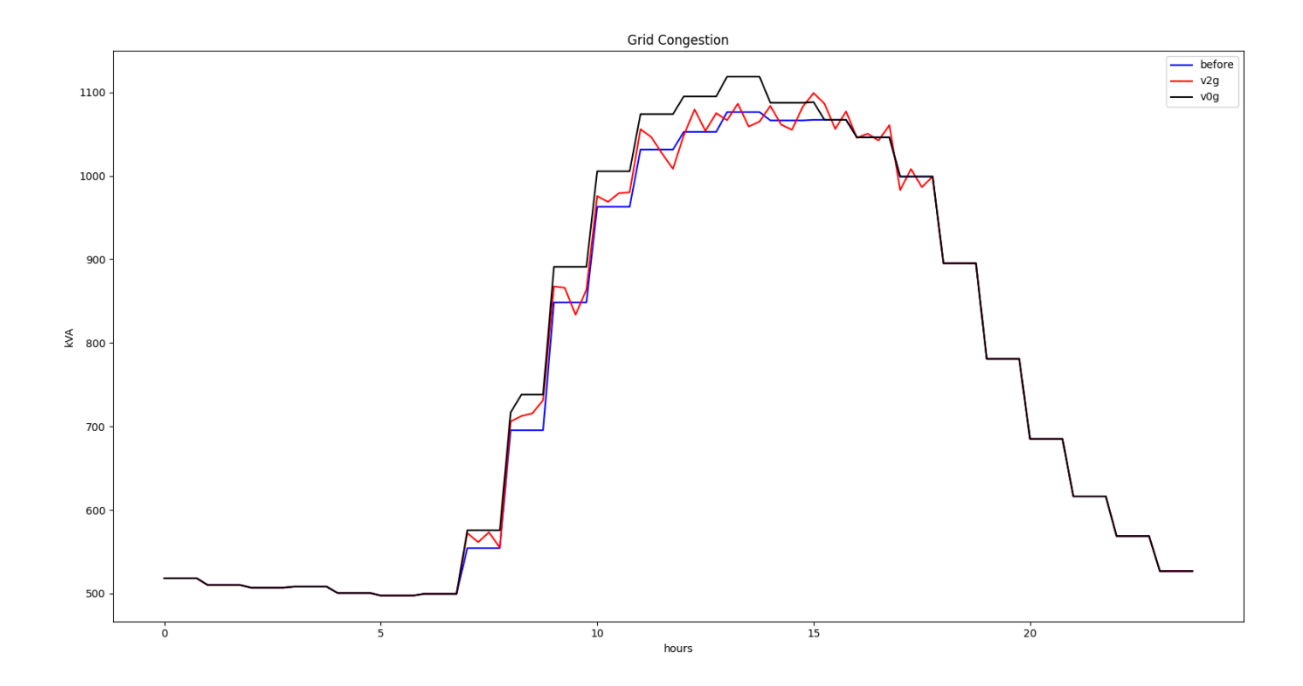


Figure 47. Central Substation loading time-series.

Additionally, through the application of the proposed solution in every transport scenario an improvement of the congestion is also evident. As shown in Figure 47 above, where the loading of the central substation of the tested grid is presented, while handling the original grid load (red), if the proposed EV chargers were to operate under V0G mode, i.e. without smart charging or discharging (blue) and in V2G mode (black). This presents the University charging scenario, but is representative for all of the 9 scenarios, since the outcome is similar for all of them.

10.4 V2G dynamic models

10.4.1 Application overview

In the context of SCALE T5.2, CERTH has utilised the component models documented in D2.6 (20, 2025) to create a representation of the Gothenburg MV grid through a new system model. More specifically, the component models of CERTH's in-house INTEMA.grid simulator are utilised to represent power system dynamic operation. These models are developed using Modelica, an equation-based multi-domain modelling language, used for the representation of physical systems. Customised component models for generators, EV powertrain and bidirectional V2G charger developed by CERTH (refs.24-27, 2024) are combined with the open-source library PowerSystems (28, 2015 and 29,2025). Three-phase AC system representation is accomplished through dq0 models, while the EV battery is modelled using the well-established technique of equivalent circuit model (ECM) to accurately capture nonlinear effects and performance dependencies on variable conditions (e.g., SoC, operating temperature). V2G charger model draws on the P/Q control mode, typically used in grid-connected energy storage systems (ESS).

To stress-test the optimal EVCI rollout topology proposed in the previous step of Energy Planning Tool, 24-hour simulations have been conducted according to the setpoint values, as provided by the optimal dispatch schedule and the system response is monitored. Based on the 9 different transport scenarios and the corresponding proposed EVCI topology, 9 separate models have been designed. Indicatively, the system



model created for scenario 5 is presented in Figure 48. Models are used for the dynamic simulation of the Chalmers MV DN following the installation of the chargers on the proposed positions. Detailed results per scenario are included in the next paragraphs. Historical data of the power consumption have been provided for each line load by Chalmers University of Gothenburg, whose campus is used as a real-life demonstrator. This is a MV DN and the transformers (MV/LV) are considered as loads. The DN is connected to a bus that can be considered as a slack bus, according to the operator's instructions.

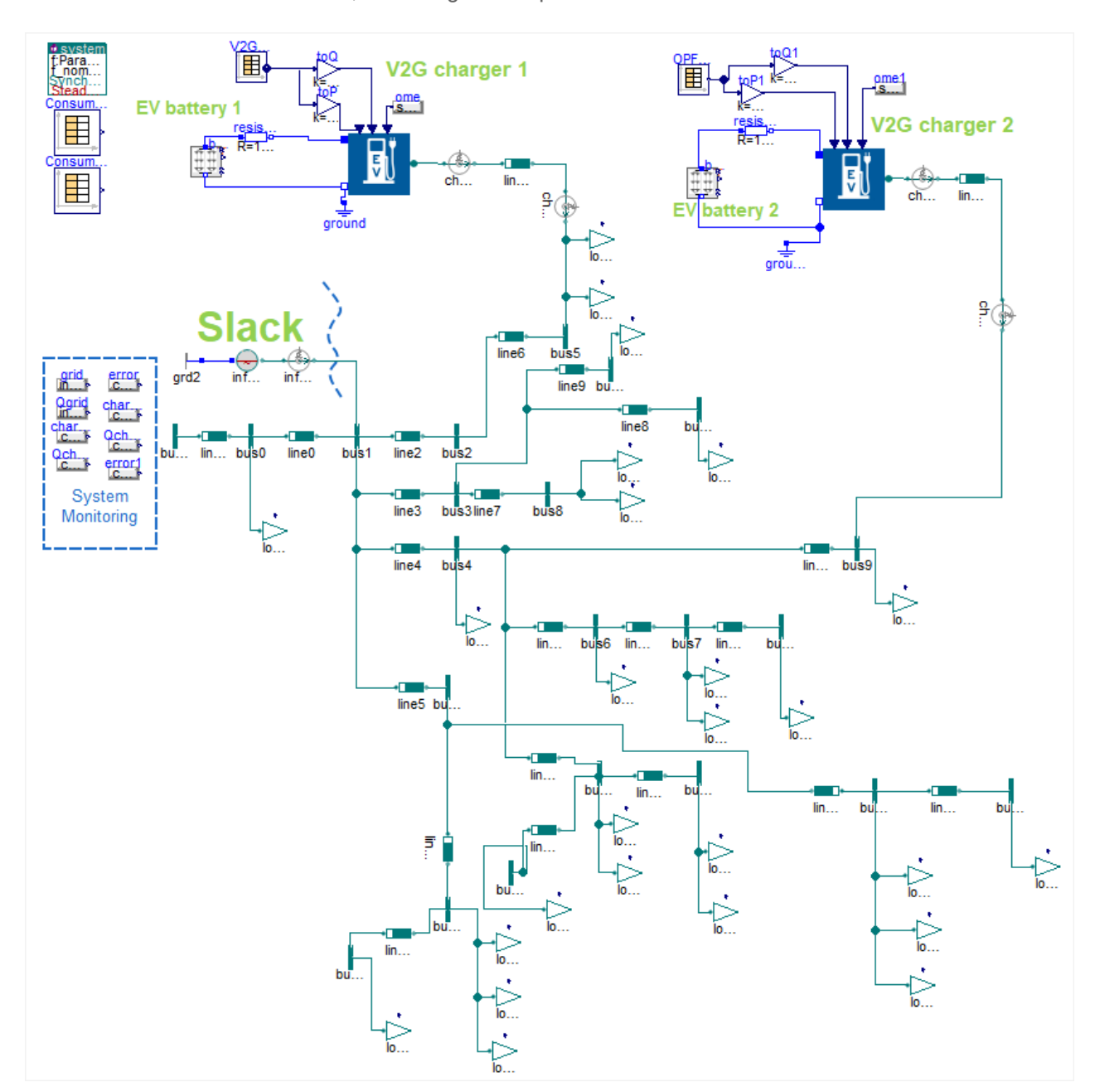


Figure 48: Chalmers campus power system model for transport scenario 5

10.4.2 Results

This section presents some key results of the simulations. The objective of this application is to verify the correct modelling of V2G chargers in a MV DN, with a particular focus on the successful implementation of



P/Q control – i.e., the ability of the inverter to adjust its output so that active and reactive power injection or absorption follows the setpoints defined by the optimal dispatch schedule from the previous optimisation step. This process effectively serves as a test of the grid's dynamic operation and responsiveness under a day-ahead energy planning scheme, offering valuable insights to DSOs about grid services enabled by EVCI.

Figure 49 presents, indicatively for Scenarios 1, 3, and 6, the trajectory of the active power supplied by the V2G chargers to the grid, compared against the setpoint values from the optimal scheduling process described in the previous section. In all cases, the EV chargers successfully inject or absorb the requested active power to or from the grid, closely following the desired trajectory. The key modelling challenge lies in ensuring that the charging infrastructure's control system can accurately regulate the output to match the optimal dispatch schedule. The resulting error in all scenarios is minimal, representing a negligible percentage of the requested power.



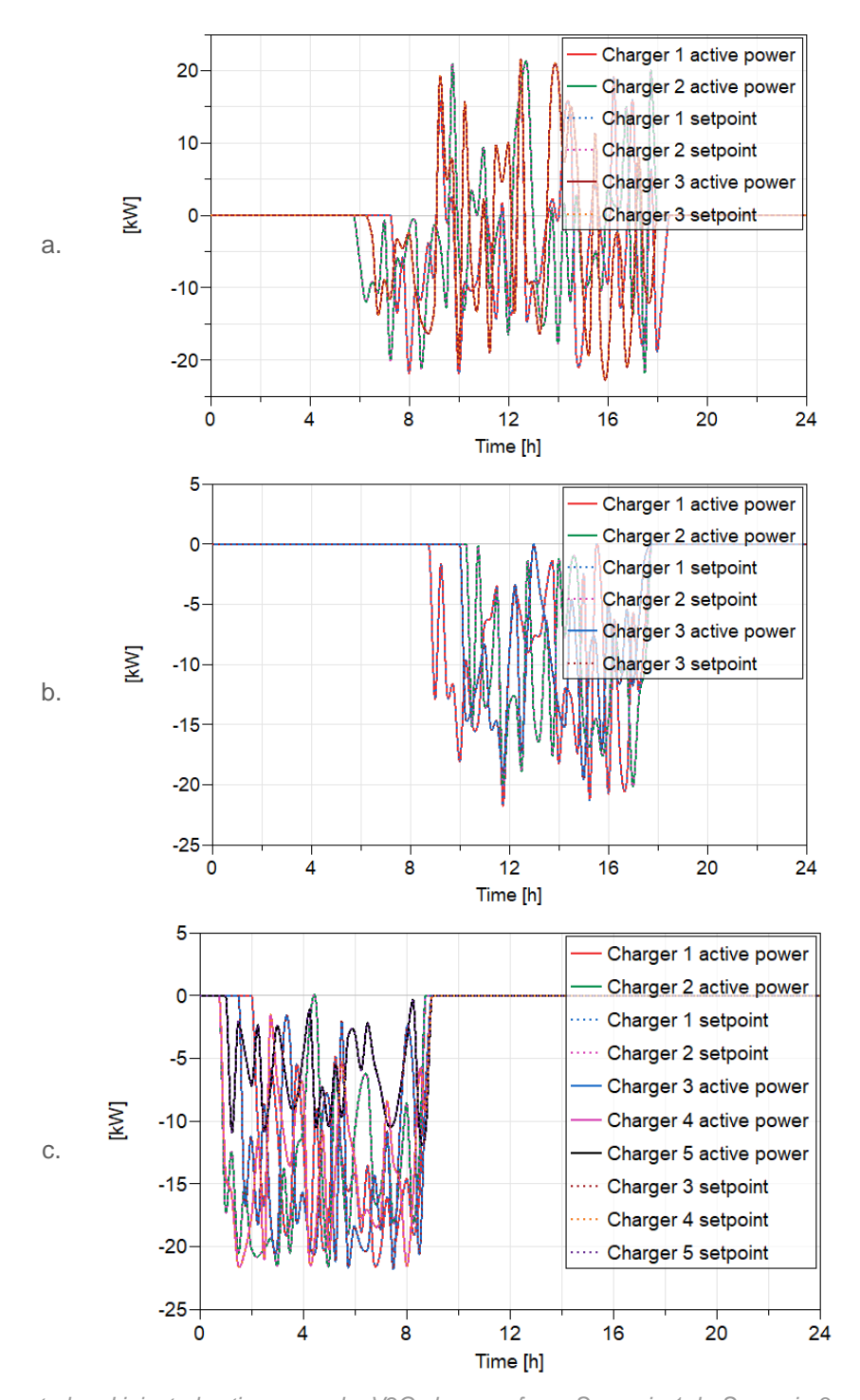


Figure 49: Requested and injected active power by V2G chargers for a. Scenario 1, b. Scenario 3 and c. Scenario 6

The evaluation of the technical feasibility of the proposed charging infrastructure topology and power dispatch schedule includes assessing whether critical system variables remain within acceptable operating limits. These variables include grid voltage magnitude and angle, as well as EV battery voltage and SoC.

In all scenarios, the voltage response at selected buses (0, 5, 11, and 20, as defined by the Energy Planning Tool and the V2G charger connection points) is monitored and shown in Figure 50. The voltage magnitude remains consistently within the acceptable operating limits – above 0.9991 p.u. – throughout the 24-hour



simulation period, indicating stable operation. This minimal voltage deviation reflects proper controller tuning under simulation conditions and confirms that the integration of V2G chargers does not negatively impact grid voltage stability. This is important from the side of the grid consumer.

It should be noted that frequency stability and system-wide voltage reference are maintained by the slack bus, which is modeled as an infinite bus. As such, no emphasis is placed on analysing frequency dynamics in this study. Additionally, the power levels of the installed V2G chargers (11–22 kW each) are negligible compared to the total system loading (2–5 MW). Therefore, their impact to large-scale dynamic effects such as frequency regulation is limited in this context. A more detailed investigation into frequency stability or grid-forming behavior from EV battery systems would be more relevant in studies of higher V2G penetration or in islanded grid conditions – topics that lie outside the scope of this specific study but are addressed in Section 9.

The focus here is on the accurate representation all components within the scope of application, including the charging infrastructure, power converters, and the EV batteries, as well as on verifying that the system model can effectively monitor key variables throughout operation. EV battery performance remains within allowable limits, and SoC is tracked in all scenarios, with Figure 51 showing results for EV #1 in Scenario 1. The nonlinear voltage response as a function of SoC is captured using an equivalent circuit model (ECM), allowing for accurate estimation of battery voltage. This modelling fidelity is critical for charging infrastructure designers and DSOs, who must consider EV-specific technical constraints during planning. Figure 51 presents EV battery pack voltage results for EV #1 in Scenario 1.

Overall, the results confirm the technical feasibility of the proposed EVCI layout and V2G scheduling across all examined mobility patterns, demonstrating stable grid behaviour and consistent performance at the component level throughout the simulations.



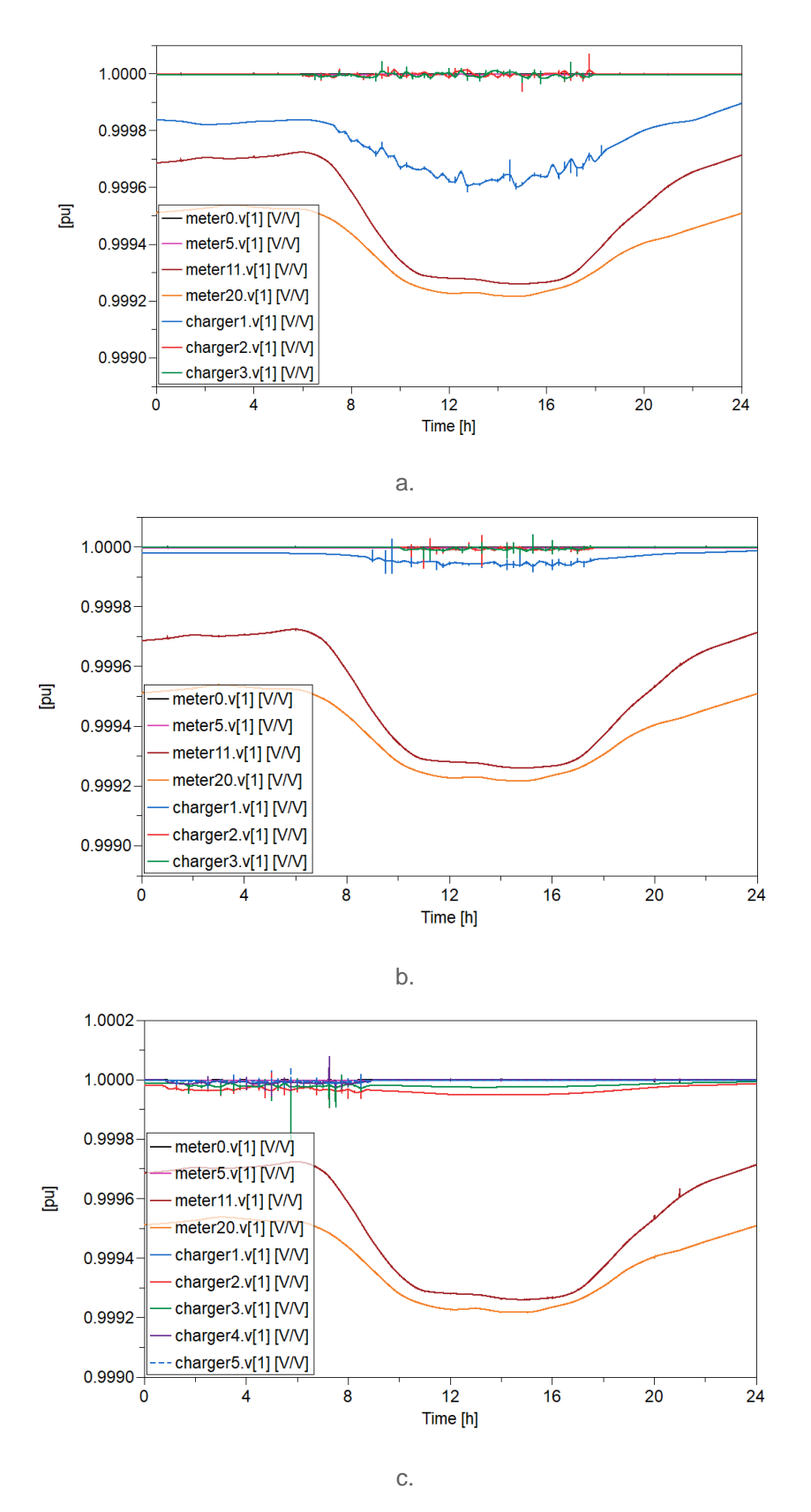


Figure 50: Voltage magnitude evolution for a. Scenario 1, b. Scenario 3 and c. Scenario 6



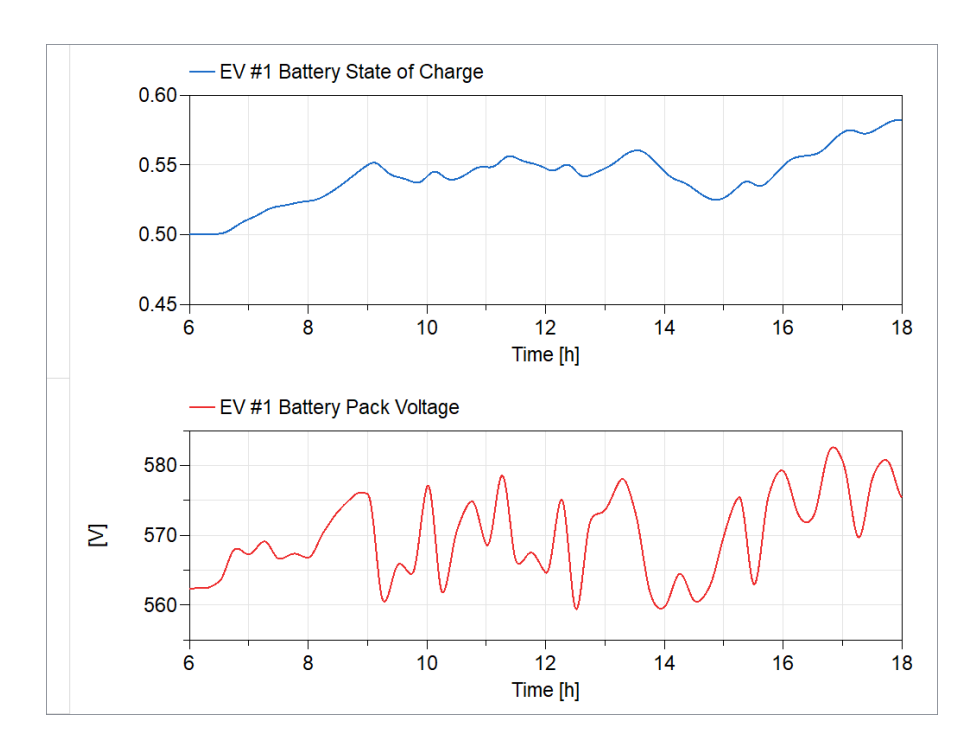


Figure 51: Evolution of EV #1 battery state of charge and pack voltage in Scenario 1

10.5 Remarks on the application of Energy Planning tool in the Gothenburg Pilot

In conclusion, the analysis of various charging scenarios reveals distinct patterns of electric vehicle usage, each reflecting different temporal and spatial charging behaviours. From workplace charging with its predictable daily cycles to public and event-based charging, these scenarios cover a broad spectrum of potential use cases. The residential charging scenario is particularly significant, as it highlights the importance of overnight charging in supporting daily commuter needs, while fast charging stations and fleet charging emphasize the necessity for quick turnaround times and flexibility. Other scenarios, such as university campus and hotel charging, reflect the changing demands based on time of day and location, offering insights into how different spaces contribute to overall grid load and EV integration. By modelling these scenarios, we can identify key strategies to optimize grid performance, enhance charging efficiency, and contribute to a sustainable and flexible energy system capable of accommodating the growing adoption of electric vehicles.

The Energy Planning Tool developed by CERTH proves its extendibility to MV DNs through testing with actual measurements and design specifications of a local DN in Gothenburg. The results show that the most desirable locations for placing EV chargers are close to the central substation, regardless of the EV transport -charging scenarios, avoiding congestion and reducing grid losses as much as possible.

An overall evaluation of the dynamic simulations demonstrates that EV battery performance remains within allowed operating limits while V2G controllers is following the proposed EVCI rollout scheduling. Moreover, the proposed technology is approved in terms of technical feasibility since system stability is secured.



11 Conclusions

PART A)

The project explored both local and system-wide impacts of EV integration, focusing on energy management, grid stability, and frequency control. At the household level, market algorithms for V1G and V2G charging were developed, optimizing energy use by considering home consumption, PV generation, driving patterns, and electricity prices. The findings highlight V2G's potential to enhance self-consumption of RES, reduce peak demand, and improve overall energy efficiency. However, power flow analyses on distribution grids revealed that while EV charging guided by market signals can support voltage stability, excessive charging or discharging may cause voltage issues, especially in grids with unbalanced PV integration. To mitigate these risks, a solution was proposed in the form of automatic PCC tap control as a function of critical cable loading, demonstrating its effectiveness in stabilizing voltage and enabling safer EV integration.

Relating to the possibilities to improve the operation of the high-voltage transmission system, EVs were integrated into the NPS test model and utilized for FCR-D services, demonstrating their ability to provide fast and effective frequency support. Unlike traditional hydro generators, EVs—through power electronic converters—offer a quicker response, improving frequency stability and damping oscillations. The study quantified the necessary EV power contributions under different control scenarios. It was assumed that other reserves, such as HVDC, RES, and loads, were not included, so the EVs were purposely stressed to highlight their dynamic properties. A critical finding was the impact of control delays in EV frequency response. While delays up to 0.5 seconds may still meet FCR-D requirements, they introduce risks of small-signal instability when large EV control gains are applied, emphasizing the need for careful assessment of control system delays to ensure grid stability.

PART B)

The application of the Energy Planning Tool in a campus DN of Chalmers University of Technology within the SCALE pilot in Gothenburg has demonstrated the tool's robustness in addressing V2G deployment under realistic mobility and grid conditions. By combining transport modelling, optimisation of charging infrastructure siting, and dynamic grid simulations, the study validated the technical feasibility of coordinated V2G integration in a MV-level DN. The scenario-based analysis revealed how different usage patterns affect grid performance and highlighted the importance of strategic charger placement to reduce losses and avoid congestion. Moreover, the dynamic system evaluation confirmed that V2G controllers can reliably track scheduled power exchange without compromising EV battery integrity or grid stability. These findings support the scalability of the tool and its relevance for guiding DSO decision-making in future EV infrastructure rollouts.



12 References

- 1. Pandapower software tool. Retrieved on 05-20-2025 from: https://www.pandapower.org/
- 2. Pymoo software tool. Retrieved on 05-20-2025 from: https://pymoo.org/
- 3. J. Einolander, A. Kiviaho and R. Lahdelma (2023). Household Electricity Cost Optimization with Vehicle-to-Home Technology and Mixed-Integer Linear Programming. International Conference on Future Energy Solutions.
- 4. J. Einolander and R. Lahdelma (2022). Explicit demand response potential in electric vehicle charging networks: Event-based on the mutivariate copula procedure. Energy, Volume 256, pp. 124656.
- 5. J. Salpakari, T. Rasku, J. Lindgren and P. D. Lund (2017). Flexibility of electric vehicles and space heating in net zero energy houses: an optimal control model with thermal dynamics and battery degradation. Applied Energy, Volume 190, pp. 800-812.
- 6. T. Kern, P. Dossow and E. Morlock (2022). Revenue opportunities by integrating combined vehicle-to-home and vehicle-to-grid applications in smart homes. Applied Energy, Volume 307, pp. 118187.
- 7. R. Khezri, D. Steen and L. A. Tuan (2023). Optimal EV Charge Scheduling Considering FCR Participation and Battery Degradation. IEEE International Conference on Energy Technologies for Future Grids (ETFG).
- 8. P. Astero and C. Evens (2021). Optimum day-ahead bidding profiles of electrical vehicle charging stations in FCR markets. Electric Power System Research. Volume 190, pp. 106667.
- 9. N. Hatziargyriou et al. (2021). Definition and Classification of Power System Stability Revisited & Extended. IEEE Transactions on Power Systems. Volume 36, Number 4, pp. 3271-3281.
- 10. D. Obradović (2024). Doctorate thesis: Coordinated Frequency Control Using DC Interconnections Between AC Systems. Stockholm: KTH Royal Institute of Technology.
- 11. ENTSO-E (2019). Fast Frequency Reserve Solution to the Nordic inertia challenge. Retrieved on 03-03-2025 from https://www.statnett.no/globalassets/for-aktorer-i-kraftsystemet/utvikling-av-kraftsystemet/nordisk-frekvensstabilitet/ffr-stakeholder-report_13122019.pdf
- 12. ENTSO-E (2023). Technical Requirements for Frequency Containment Reserve Provision in the Nordic Synchronous Area. Retrieved on 03-03-2025 from https://www.svk.se/siteassets/aktorsportalen/bidra-med-reserver/om-olika-reserver/fcr/fcr-technical-requirements-may-23.pdf
- 13. Nordic TSOs (2023). Nordic Grid Development Perspective 2023. Retrieved on 03-03-2025 from https://www.svk.se/siteassets/om-oss/rapporter/2023/svk ngpd2023.pdf
- ENTSO-E (2024). ENTSO-e grid maps: Northen Europe. Retrieved on 03-03-2025 from https://eepublications/maps/2024/ENTSOE_Grid_Map_Northern_Europe.pdf
- 15. Nordic RCC (2023). Annual Report 2023. Retrieved on 03-03-2025 from https://nordic-rcc.net/wp-content/uploads/2024/05/NordicRCC_AYReport23_A4_opslag_Web_opt-a.pdf
- 16. M. A. Kambagiri, D. Obradović, M. Persson (2025). Nordic-44-model-for-SCALE. GitHub repository. Available: https://github.com/Mahantha-Ak/Nordic-44-model-for-SCALE
- 17. S. Hofsmo, J. Lester, K. Espen, and H. Solvang (2018). The Nordic 44 test network. Retrieved on 03-03-2025 from https://figshare.com/articles/journal_contribution/The_Nordic_44_test_Network/7464386/1?file=138
- 18. M. A. Kambagiri (2023). Master thesis: Large Scale V2G Simulations for Frequency Stability. Gothenburg: Chalmers University of Technology.



- 19. S. Skogerstad, I. Postlethwaite (2005). Multivariable Feedback Control: Analysis and Design. John Wiley.
- 20. SCALE D2.6 (2025). Integrated EV mobility and energy planning tools. Retrieved on 04-08-2025 from:
 - https://ec.europa.eu/research/participants/documents/downloadPublic?documentIds=080166e5129 f23ab&appId=PPGMS
- 21. J. Blank and K. Deb, pymoo: Multi-Objective Optimization in Python, in IEEE Access, vol. 8, pp. 89497-89509, 2020, doi: 10.1109/ACCESS.2020.2990567.
- 22. L. Thurner et al. (2018). pandapower an Open Source Python Tool for Convenient Modeling, Analysis and Optimization of Electric Power Systems. IEEE Transactions on Power Systems, doi:10.1109/TPWRS.2018.2829021.
- 23. P.A. Gkaidatzis et al. (2024). Optimal EV Charger Placement Considering Technical Uncertainties. 2024 IEEE PES Innovative Smart Grid Technologies Europe (ISGT EUROPE), Dubrovnik, Croatia. doi: 10.1109/ISGTEUROPE62998.2024.10863260.
- 24. N. Skopetou et al. (2024). Energy Analysis and Environmental Impact Assessment for Self-Sufficient Non-Interconnected Islands: The Case of Nisyros Island. Journal of Cleaner Production, doi:10.1016/j.jclepro.2024.141647.
- 25. R. Rotas et al. (2024). Dynamic Battery Modeling for Electric Vehicle Applications. Batteries, doi:10.3390/batteries10060188.
- R. Rotas et al. (2024). Evaluating Synergies between Electric Vehicles and Photovoltaics: A Comparative Study of Urban Environments. World Electric Vehicle Journal. doi:10.3390/wevj15090397.
- 27. R. Rotas et al. (2024). Vehicle-to-Grid Dynamic Modeling in a Neighborhood of Utrecht Municipality. 2024 IEEE PES Innovative Smart Grid Technologies Europe (ISGT EUROPE), Dubrovnik, Croatia. doi: 10.1109/ISGTEUROPE62998.2024.10863639.
- 28. R. Franke et al. (2014). Flexible Modeling of Electrical Power Systems -- the Modelica PowerSystems Library. The 10th International Modelica Conference, Lund, Sweden. doi: 10.3384/ecp14096515.
- 29. https://github.com/modelica-3rdparty/PowerSystems (2025).



13 Annex

The Annex describes data relating the NPS test model used in Section 9.3.

Table 18 lists data related to the synchronous generators applied in the NPS test model.

Table 18: The list of **synchronous generators** in the NPS test model with the indication of bus number connection, name, active power output, the maximum active power out, base power, inertia constant, and indication if it is an FCR-D unit, respectively from left to right.

Number	Bus number	Bus name	Power output (MW)	Maximum active power (MW)	Base Power (MVA)	Inertia constant (s)	FCR-D
1	3115	PORJUS	1175	1306	1450	3.21	yes
2	3115	PORJUS	1175	1306	1450	3.21	yes
3	3115	PORJUS	1175	1306	1450	3.21	yes
4	3245	JARPSTROMMEN	1000	1111	1235	2.24	
5	3359	RINGHALS	1100	1217	1350	3.27	
6	3359	RINGHALS	1100	1217	1350	3.27	
7	3359	RINGHALS	1100	1217	1350	3.27	
8	5100	TRETTEN	972	1100	1200	2.71	
9	5300	SIMA	1276	1417	1575	2.37	
10	5300	SIMA	1276	1417	1575	2.37	
11	5400	OSLO1	1305	1450	1611	2.78	yes
12	5400	OSLO1	1305	1450	1611	2.78	yes
13	5500	OSLO2	900	1280	1450	1.02	
14	5600	KRISTIANSAND	1246	1384	1538	2.37	
15	5600	KRISTIANSAND	1246	1384	1538	2.37	
16	6000	KVILLDAL	736	817	897	2.37	
17	6100	BLAFALLI	1329	1477	1635	2.03	



18	6100	BLAFALLI	1329	1477	1635	2.03	
19	6100	BLAFALLI	1329	1477	1635	2.03	yes
20	6100	BLAFALLI	1329	1477	1635	2.03	yes
21	6100	BLAFALLI	1329	1477	1635	2.03	yes
22	6700	ROSSAGA	1753	1930	2145	2.43	yes
23	6700	ROSSAGA	1753	1930	2145	2.43	yes
24	7100	OULU	715	900	1000	2.17	yes
25	7100	OULU	715	900	1000	2.17	yes
26	7100	OULU	715	900	1000	2.17	
27	8500	MALMO	994	1183	1300	4.74	
28	3000	FORSMARK	1100	1167	1300	2.98	
29	3000	FORSMARK	1100	1167	1300	2.98	
30	7000	HELSINKI	1086	1167	1278	2.75	
31	7000	HELSINKI	1086	1167	1278	2.75	

The table below provides the basic wind power data utilized in the NPS test model.

Table 19: The list of **wind power** in the NPS test model with the indication of bus number connection, name, active power output, the maximum active power out, and base power.

Number	Bus number	Bus name	Power output (MW)	Maximum active power (MW)	Base Power (MVA)
1	3249	GRUNDFORS	1042	1230	1357
2	3249	GRUNDFORS	1042	1230	1357
3	3249	GRUNDFORS	1042	1230	1357
4	3249	GRUNDFORS	1042	1230	1357
5	3249	GRUNDFORS	1042	1230	1357



6	3249	GRUNDFORS	1042	1230	1357
7	3249	GRUNDFORS	1042	1230	1357
8	6500	TRONDHEM	814	1000	1100
9	6500	TRONDHEM	814	1000	1100
10	6500	TRONDHEM	814	1000	1100
11	3300	OSKARSHAMN	646	1000	1100
12	3300	OSKARSHAMN	646	1000	1100
13	3300	OSKARSHAMN	646	1000	1100
14	7000	HELSINKI	1086	1167	1278
15	7000	HELSINKI	1086	1167	1278
16	7000	HELSINKI	1086	1167	1278
17	7000	HELSINKI	1086	1167	1278

The table below lists the parameters of the governor-turbine system of the hydro FCR-D units.

Table 20: HYGOV-TUR model parameters of the hydro FCR-D units in the NPS test model.

FCR-D HYGOV parameters equally distributed among 12 generators in the NPS test model.							
Permanent droop R	Wash-out droop time constant T_r	Transient droop r	Filter time constan T_f	Rate of change of power limit on gate V_{elm}	Max turbine power limit on gate G_{max}	Min turbine power limit on gate G_{min}	
0.1	6.4 s	0.125	0.05 s	0.1 pu/s	1 pu	0 pu	
Servo time constant T_g	Turbine damping to speed change D_{tur}	Water time constant T_W	Turbine scaling gain A_t	No-load flow at nominal head $q_{\it NL}$	Head available at dam H_{dam}	Dead-band for FCR-D control	
2 s	0 pu	1.5 s	1	0.1 pu	1 pu	±0.1 Hz	

WWW.SCALE.EU ______ 74



The table below lists basic data related to the equivalent representation of the EV batteries utilized in the NPS test model.

Table 21: The list of equivalent EV **batteries** in the NPS test model with the indication of bus number connection, name, active power output, and base power.

Case	Bus number	Bus name	Power output (MW)	Base Power (MVA)
1	3100	HJALTA	Initially zero	Dependent on the
2	3115	PORJUS	2010	study case - larger
3	3200	TENHULT		gains would
4	3244	HOGASEN		require larger MW
5	6100	BLAFALLI		capacity
6	6500	TRONDHEM		
7	7100	OULU		